

1 **A Novel Methodology for Assessing the Hygroscopicity of Aerosol Filter Samples**

2 **Nagendra Raparathi¹, Anthony S. Wexler^{1,2,3,4}, Ann M. Dillner¹**

3 ¹Air Quality Research Center, University of California, Davis, 95616 CA, USA

4 ²Mechanical and Aerospace Engineering, University of California, Davis, 95616 CA, USA

5 ³Civil and Environmental Engineering, University of California, Davis, 95616 CA, USA

6 ⁴Land, Air, and Water Resources, University of California, Davis, 95616 CA, USA

7

8 *Correspondence to:* Ann M. Dillner (amdillner@ucdavis.edu)

9

10

11

12

13

14

15

16

17

18

19

20

21

22

23

24

25

26 **Abstract**

27 Due to US regulations, concentrations of hygroscopic inorganic sulfate and nitrate have declined
28 in recent years, leading to an increased importance in the hygroscopic nature of organic matter
29 (OM). The hygroscopicity of OM is poorly characterized because only a fraction of the multitude
30 of organic compounds in the atmosphere are readily measured and there is limited information on
31 their hygroscopic behaviours. ~~—Hygroscopicity of aerosol is traditionally measured using~~
32 ~~Humidified Tandem Differential Mobility Analyzer (HTDMA) or Electrodynamic Balance~~
33 ~~(EDB). EDB measures water uptake by a single particle. For ambient and chamber studies,~~
34 ~~HTDMA measurements provide water uptake and particle size information but not chemical~~
35 ~~composition. To fill in this information gap, we have developed a novel methodology to assess the~~
36 ~~water uptake by particles collected on Teflon filters. This method uses the same filter sample for~~
37 ~~both hygroscopicity measurements and chemical characterization, thereby providing an~~
38 ~~opportunity to link the measured hygroscopicity with ambient particle composition.~~~~For ambient~~
39 ~~and chamber studies, HTDMA measurements provide water uptake and particle size information~~
40 ~~but not chemical composition. To fill in this information gap, we have developed a novel~~
41 ~~methodology to assess the water uptake of particle collected on Teflon filters, thereby providing~~
42 ~~an opportunity to link the measured hygroscopicity with ambient particle composition.~~ To test the
43 method, hygroscopic measurements were conducted in the laboratory for ammonium sulfate,
44 sodium chloride, glucose, and malonic acid, which were collected on 25mm Teflon filters using
45 an aerosol generator and sampler. Constant humidity solutions (CHS), including potassium
46 chloride, barium chloride dihydrate, and potassium sulfate, were employed in the saturated form
47 to maintain the relative humidity (RH) at approximately 84%, 90%, and 97% in small chambers.
48 Our preliminary experiments revealed that, without the pouch, water uptake measurements were
49 not feasible due to rapid water loss during weighing. Additionally, we observed some absorption
50 by the aluminum pouch itself. To account for this, concurrent measurements were conducted for
51 both the loaded and blank filters at each RH level. Thus, the dry loaded and blank Teflon filters
52 were placed in aluminum pouches with one side open and placed in RH-controlled chambers for
53 more than 24 hours. The wet-loaded samples and wet blanks were then weighed using an
54 ultramicrobalance to determine the water uptake by the respective compound and the blank Teflon
55 filter. The net amount of water absorbed by each compound was calculated by subtracting the
56 water uptake of the blank filter from that of the wet-loaded filter.~~Constant humidity solutions~~

57 ~~(CHS) were employed to maintain the relative humidity (RH) at approximately 84%, 90%, and~~
58 ~~97% in small chambers.~~ Hygroscopic parameters, including the water-to-solute (W/S) ratio,
59 molality, mass fraction solute (mfs), and growth factors (GF), were calculated from the
60 measurements. The results obtained are consistent with those reported by the E-AIM model and
61 previous studies utilizing HTDMA and EDB for these compounds, highlighting the accuracy of
62 this new methodology. This new approach enables the hygroscopicity and chemical composition
63 of individual filter samples to be assessed so that in complex mixtures such as chamber and
64 ambient samples, the total water uptake can be parsed between the inorganic and organic
65 components of the aerosol.

66 **Keywords:** Hygroscopicity, Organic Aerosol, Teflon Filters, Constant Humidity Solutions

67
68
69
70
71

72 **Highlights**

- 73 • This is the first study to assess the hygroscopicity of particles collected on Teflon filters at
74 near-saturation levels using constant humidity solutions.
- 75 • This study's methodology can evaluate water uptake at RH levels as high as ~97%.
- 76 • This methodology enables the investigation of composition-dependent hygroscopicity of
77 particles.

78
79
80
81
82
83

84
85
86
87
88
89
90
91
92
93
94
95
96
97

1. Introduction

98 Atmospheric particles significantly degrade air quality by reducing visibility and posing health
99 risks to humans (Gupta et al., 2022; Kohli et al., 2023; Qu et al., 2020). Additionally, they function
100 as cloud condensation nuclei (CCN) or ice-nucleating particles (INPs), profoundly influencing
101 cloud properties and consequently exerting a significant effect on Earth's radiation budget (Haseeb
102 et al., 2024; Lee et al., 2008; Li et al., 2022; Mikhailov et al., 2021; Nadler et al., 2019; Reich et
103 al., 2023; Sjogren et al., 2007; K. Wang et al., 2021; Zieger et al., 2017). Atmospheric aerosol
104 consists of both organic and inorganic compounds with varying physicochemical properties, which
105 further determine the CCN activity, reactivity, deposition, and optical properties (Padró et al.,
106 2012; J. Wang et al., 2010). Historically, the hygroscopic (water-attracting) characteristics of CCN
107 were primarily influenced by inorganic compounds such as nitrates, sulfates, and chlorides.
108 However, with the implementation of emissions controls that have successfully reduced nitrogen
109 and sulfur oxide emissions, the organic fraction of aerosol is assuming a more prominent role.

110 Additionally, the organic fraction is considerably more complex than its inorganic counterpart,
111 comprising thousands of individual compounds originating from diverse sources and reaction
112 pathways, each possessing distinct physical and chemical properties (Boris et al., 2019; Jathar et
113 al., 2016). This complexity often poses challenges to establishing a clear correlation between the
114 organic fraction and hygroscopicity (Han et al., 2022).

115 The hygroscopicity of particles, which refers to their ability to absorb water, depends on both size
116 and chemical composition (Luo et al., 2020; Zieger et al., 2017). The water activity of atmospheric
117 particles, particularly the affinity of various solutes for water, plays a crucial role in governing
118 several important factors. These include the “total mass concentration of airborne particles, their
119 acidity, the extent of light scattering, their rates of aqueous phase chemical reactions, and their
120 ability to act as cloud condensation nuclei (CCN)” (Saxena et al., 1995). To characterize these
121 attributes of airborne particles, it is necessary to know the amount of water uptake as a function of
122 particle composition and relative humidity (RH) (Saxena et al., 1995).

123 Various thermodynamic models are available for estimating hygroscopicity, including,
124 ISORROPIA (Nenes et al., 1998), Aerosol Inorganic-Organic Mixtures Functional groups Activity
125 Coefficients (AIOMFAC) (Zuend et al., 2010), Extended Aerosol Inorganic Model (E-AIM)
126 (Clegg et al., 1998), Universal Quasi-Chemical Functional group Activity Coefficients (UNIFAC)
127 model (Fredenslund et al., 1975), and the University of Manchester System Properties
128 (UManSysProp) (Topping et al., 2016). For the organics, they utilize group contribution methods
129 to estimate the water activity of ambient species relevant to the atmosphere (Han et al., 2022).
130 However, these models require further experimental data to validate them and refine their
131 predictions (Han et al., 2022).

132 Various techniques exist to measure the hygroscopic growth of aerosol particles. These include
133 methods such as the Humidifier Tandem Differential Mobility Analyzer (HTDMA),
134 Electrodynamic Balance (EDB), Differential Aerosol Sizing and Hygroscopicity Probe (DASH-
135 SP), and direct mass measurements of water uptake by particles collected on aerosol filters. These
136 techniques have been extensively reviewed in previous studies by Kreidenweis & Asa-Awuku
137 (2014) and Tang et al. (2019). Among these, the most employed methods are the HTDMA
138 (Boreddy et al., 2014; Laskina et al., 2015; Mikhailov et al., 2021) and EDB (Chan et al., 1992,
139 2000; Cohen et al., 1987; Kohli et al., 2023; Peng et al., 2001; Steimer et al., 2015; Tang &

140 Munkelwitz, 1991). EDB measures the change in mass of individual charged particles of known
141 composition, which are levitated in a gaseous atmosphere by means of an electric field created by
142 imposing voltages on the electrodes (Cohen et al., 1987; Kohli et al., 2023). When the mass of a
143 levitating particle undergoes evaporation or condensation due to a change in RH, it becomes
144 proportional to the DC voltage required to balance the particle in a stationary position. The
145 particle's mass fraction of the solute (mfs) can then be determined by measuring the particle's
146 balancing voltage with that of a reference state of known composition (Peng et al., 2001).
147 However, EDB is limited to analyzing single particles and is not suitable for studying the water
148 uptake of ambient samples. HTDMA measures the change in particle size distribution in response
149 to varying humidity levels and can be used to measure ambient aerosol. By exposing aerosol
150 particles to controlled humidity levels and measuring their sizes before and after exposure,
151 HTDMA assesses the extent of hygroscopic growth as a function of particle size. This method
152 measures the change in the diameter of the particles, from which parameters such as mfs and solute
153 molality are estimated. However, this method faces challenges in measuring RH conditions
154 exceeding 90% (Marsh et al., 2019), an RH regime that can lead to very high water uptake and is
155 not applicable for measuring the hygroscopicity of particles collected on aerosol filters. An
156 alternative to HTDMA is the DASH-SP, which can measure hygroscopic growth at RH levels as
157 high as 95% and perform rapid, size-resolved measurements of subsaturated particle
158 hygroscopicity (Shingler et al., 2016; Sorooshian et al., 2008). However, DASH-SP is impractical
159 for measuring the hygroscopicity of particles collected on filters.

160 Quartz crystal microbalances (QCMs) offer a direct method for measuring water uptake by aerosol
161 particles collected on filters. These instruments utilize the Sauerbrey equation to quantify mass-
162 based hygroscopic behavior of particulate matter (Tang et al., 2019 and reference therein). Jose et
163 al. (2024) demonstrated the application of QCM technology to measure hygroscopic growth of
164 size-resolved aerosol particles on Teflon filters at RH levels up to 93%. The experimental protocol
165 involved transferring collected particles to the QCM sensor via direct contact by placing the filter
166 onto the sensor and gently pressing it with a cotton piece. However, the Sauerbrey equation's
167 accuracy may be compromised when the deposited film lacks rigidity or exhibits poor surface
168 coupling, potentially introducing systematic errors in hygroscopic property estimations (Tang et
169 al., 2019). Alternative methodologies, including physisorption and katharometer analyzers, have
170 been employed to quantify water vapor concentration changes resulting from particle-water

171 interactions on aerosol filters (Ma et al., 2010; Mikhailov et al., 2011). However, physisorption
172 analyzers typically necessitate substantial sample masses (≥ 1 mg), which limits their applicability
173 in atmospheric aerosol studies (Gu et al., 2017). Moreover, both physisorption and katharometer
174 techniques are characterized by extended experimental durations, often spanning several days (Gu
175 et al., 2017; Mikhailov et al., 2020). The precision of katharometer methods in quantifying water
176 adsorption within nanoscale layers remains a subject of ongoing investigation (Tang et al., 2019),
177 highlighting the need for further refinement of these analytical techniques.

178 Analytical balances have been employed to measure the mass change of particles collected on
179 aerosol filters due to water uptake under controlled conditions. For instance, McInnes et al. (1996)
180 used a semi-dynamic method to measure the water uptake of particles collected on Millipore
181 Fluoropore filters, with the microbalance housed in a chamber controlled for humidity and
182 temperature. They maintained a 33% RH using a saturated solution of $\text{MgCl}_2 \cdot 6\text{H}_2\text{O}$, with the
183 lowest RH achieved via nitrogen cylinders. The aerosol water uptake at 33% RH was calculated
184 as the difference in mass between higher and lower RH conditions. However, most organic and
185 inorganic compounds do not take up significant water at 33% RH. Similarly, Hitzenberger et al.
186 (1997) employed a semi-dynamic method to measure aerosol particles collected on aluminum
187 foils, maintaining RH levels between 45% and 95% using varying concentrations of CaCl_2
188 solutions in a housed chamber. Nevertheless, actual humidities inside the chamber were lower than
189 the water activities of the CaCl_2 solution, due to a narrow chamber opening, resulting in differing
190 growth patterns for two samples collected at the same location and time of the year (Hitzenberger
191 et al. 1997). Housing microbalances in chambers with high humidity ($> 80\%$ RH) is also
192 problematic, as the high moisture can corrode electronic components, affecting measurement
193 accuracy and stability. However, many atmospheric aerosols, especially those with deliquescence
194 relative humidities (DRH) greater than 80%, undergo rapid water uptake at RH $> 95\%$
195 (Kreidenweis & Asa-Awuku, 2014). Therefore, there is a need to develop robust laboratory
196 techniques capable of measuring composition-dependent water uptake of aerosols collected on
197 Teflon filters under near-saturated conditions. Previous studies have measured the hygroscopic
198 growth of both inorganic and organic compounds relevant to the atmosphere. Techniques such as
199 the Humidifier Tandem Differential Mobility Analyzer (HTDMA) (Boreddy et al., 2014; Laskina
200 et al., 2015; Mikhailov et al., 2021) and the Electrodynamic Balance (EDB) (Chan et al., 1992;
201 2000; Cohen et al., 1987; Kohli et al., 2023; Peng et al., 2001; Steimer et al., 2015; Tang &

Formatted: Subscript

Formatted: Subscript

202 ~~Munkelwitz, 1991) have been utilized for this purpose. EDB measures the change in mass of~~
203 ~~individual charged particles of known composition, which are levitated in a gaseous atmosphere~~
204 ~~by means of an electric field created by imposing voltages on the electrodes (Cohen et al., 1987;~~
205 ~~Kohli et al., 2023). When the mass of a levitating particle undergoes evaporation or condensation~~
206 ~~due to a change in RH, it becomes proportional to the DC voltage required to balance the particle~~
207 ~~in a stationary position. The particle's mfs can then be determined by measuring the particle's~~
208 ~~balancing voltage with that of a reference state of known composition (Peng et al., 2001).~~
209 ~~However, EDB is limited to analyzing single particles and is not suitable for studying the water~~
210 ~~uptake of ambient samples. HTDMA measures the change in particle size distribution in response~~
211 ~~to varying humidity levels and can be used to measure ambient aerosol. By exposing aerosol~~
212 ~~particles to controlled humidity levels and measuring their sizes before and after exposure,~~
213 ~~HTDMA assesses the extent of hygroscopic growth as a function of particle size. This method~~
214 ~~measures the change in the diameter of the particles, from which parameters such as mass fraction~~
215 ~~of the solute (mfs) and solute molality are estimated. However, this method does not measure~~
216 ~~chemical composition of the particles and faces challenges in measuring RH conditions exceeding~~
217 ~~90% (Marsh et al., 2019), an RH regime that can lead to very high water uptake. Therefore, there~~
218 ~~is a need to devise a laboratory technique capable of measuring composition dependent water~~
219 ~~uptake of aerosol sampled on the Teflon filters.~~

220
221 This study's objective is to devise a methodology for assessing the water uptake of organic and
222 inorganic aerosol in samples with known chemical composition. Samples collected on Teflon filter
223 are commonly used for gravimetric and chemical analysis, and we developed a method to measure
224 water uptake on the same filter enabling correlation chemical composition with hygroscopicity.
225 ~~This study's objective is to devise a methodology for assessing the water uptake of organic and~~
226 ~~inorganic aerosol collected on Teflon filters which are commonly used for gravimetric and~~
227 ~~chemical analysis. Our aim is to accurately estimate water adsorption by solute molecules that~~
228 ~~commonly act as cloud condensation nuclei (CCN), which include atmospheric relevant inorganics~~
229 ~~such as ammonium sulfate and sodium chloride, as well as organics such as glucose, a sugar, and~~
230 ~~malonic acid, a dicarboxylic acid. We compare the results obtained to data from the literature to~~
231 ~~gain insights into the accuracy of the methodology developed. The novelty of this research lies in~~

232 the development of method to determine the hygroscopicity of aerosol filter samples so that the
233 chemical composition can be measured and to measure at high relative humidity, exceeding 90%,
234 which is relevant to CCN and where most organic and inorganic compounds absorb considerable
235 amounts of water. In addition, unlike HTDMA measurements, there is no need to account for shape
236 factor of a compound, as this method directly measures the mass of water uptake by the particles
237 collected on the Teflon filters.

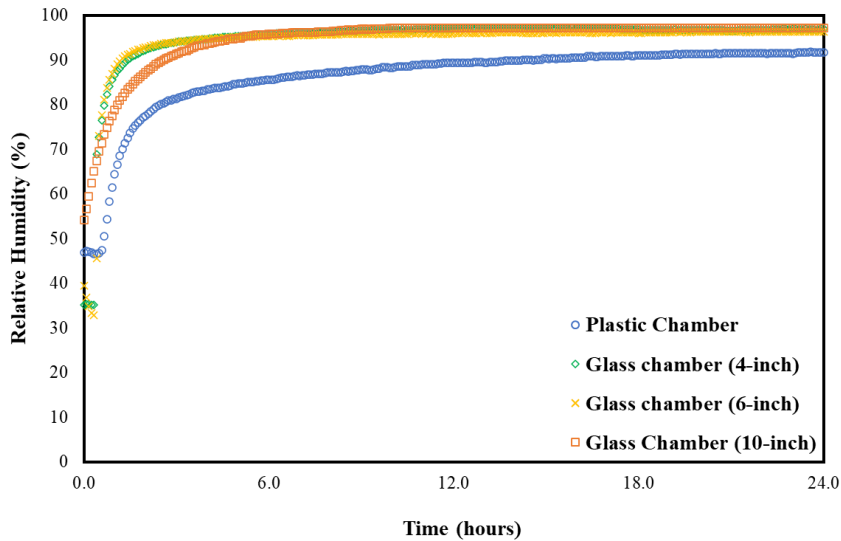
238 **2. Experimental observations**

239 **2.1. Relative Humidity Controlled Chamber**

240 The initial step in developing this methodology involves maintaining RH throughout the
241 entire water uptake measurement process. Constant humidity solutions (CHS) (Lide, 2004) offer
242 a means to sustain specified RH levels within sealed chambers. In this study, our aim was to
243 measure the water uptake of both organic and inorganic compounds across a range of high RH
244 levels above 80%. Potassium chloride, barium chloride dihydrate, and potassium sulfate were
245 selected for their capacity to maintain RH levels of approximately 84%, 90%, and 97%,
246 respectively, in their saturated form. Prior to conducting the actual water uptake measurements,
247 we placed these saturated solutions in 10-inch plastic and glass chambers for 24 hours to assess
248 their practical efficacy. In addition, a real-time RH and temperature sensor (Rotronic HL-1D, with
249 an accuracy of $\pm 3.0\%$ RH and $\pm 0.3^\circ\text{C}$) was placed inside the chambers. In the glass chambers, the
250 RH reached the desired RH levels, but not so in the plastic chambers, likely due to the absorption
251 by the plastic itself (Fig. 1). Wexler and Hasegawa (1954) specifically noted that chambers should
252 be made of non-hygroscopic materials, preferably metal or glass, as otherwise, the time required
253 to achieve RH equilibrium could be substantial, sometimes spanning days or weeks. Similar
254 observations were made in our study.

255 Next, we used 4, 6, and 10-inch diameter glass chambers, to examine the consistency of
256 RH levels across different chamber sizes. As expected, all these chambers reached their optimal
257 RH depending on the saturated solutions used but there was a difference in time to equilibration.
258 For instance, the initial time taken to reach the desired RH of $\sim 97\%$ (saturated K_2SO_4) for a 10-
259 inch chamber was slightly longer compared to 4- and 6-inch chambers (Fig. 1). Based on these
260 observations, it is evident that RH equilibrium is influenced by the presence of hygroscopic
261 materials, and the ratio of the solution's free surface area to the chamber volume. These findings

262 affirm the appropriateness of CHS for conducting water uptake measurements using glass
 263 chambers of any size and that smaller sizes equilibrate more quickly.
 264



265 **Figure 1.** RH over 24-hours in the plastic (10-inch) and glass (4, 6, and 10-inch) chamber
 266 with saturated K₂SO₄ solution
 267
 268

269 **2.1.1. Determining the RH (a_w) for the CHS**

270 In the CRC Handbook (volume 85), (Lide, (2004) provided integer RH values for CHS at
 271 25⁰C. However, even a small variation in RH could substantially affect water uptake, particularly
 272 at higher RH levels, where the water uptake change per change in RH is very steep. The average
 273 temperature during these experiments ranged from 17.9⁰C to 21.6⁰C. To evaluate the effect of
 274 temperature variation on RH, the water activity over this range was calculated for each compound
 275 used to create CHS. The water activity is ~0.843 for saturated KCl and ~0.975 for saturated K₂SO₄,
 276 with no significant variation within the temperature range, according to Eq. (1) provided by Wexler
 277 & Seinfeld (1991),

278
$$\ln \frac{a_w(T)}{a_w(T_0)} = -\frac{M_w}{1000} m_s \frac{L_s}{R} \left(\frac{1}{T} - \frac{1}{T_0} \right) \quad (1)$$

279 where $a_w(T)$ is the water activity at temperature (T), $a_w(T_0)$ is the water activity at temperature
280 (T_0 , 298.15K), M_w is the molecular weight of water (18.01528 g/mol), m_s is the saturated molality
281 of the compound used as CHS, R is the universal gas constant (8.314 kJ/kmol-K) and L_s is the
282 latent heat of fusion for the salt from a saturated solution; it equals the difference between the
283 standard heat of formation of the crystalline solid phase ($\Delta H_{f,c}$) and ($\Delta H_{f,aq}$), the standard heat of
284 formation of the species in the aqueous solution at saturation molality. For $a_w(T_0)$, the values are
285 0.8426 for KCl and 0.975097 for K_2SO_4 (Kim & Seinfeld, 1995). The average saturated molality
286 (m_s , in mol/kg) is 4.604 for KCl (Shearman & Menzis, 1937) and 0.636 for K_2SO_4 (Krumgalz,
287 2018). The latent heat of fusion (L_s , in kJ/mol) is -15.287 for KCl and -23.77 for K_2SO_4 (Kim &
288 Seinfeld, 1995).

289 The water activity for saturated $BaCl_2 \cdot 2H_2O$ was determined by extrapolating the water activities
290 provided by (X. Wang et al., 2013) at temperatures of 5, 15, 25, and 35°C (See Fig. S1). The
291 average a_w for saturated $BaCl_2 \cdot 2H_2O$ during these experiments was ~0.908, ranging from 0.906 to
292 0.911 and for each experiment the variability in RH due to temperature fluctuations in the lab was
293 negligible (less than 0.25%).

294

295 **2.2. Laboratory sample collection**

296 The laboratory particulate samples were produced utilizing a home-built aerosol generator
297 and sampler, which consists of an atomizer (Aerosol generator 3076, TSI Inc., USA), a custom-
298 built diffusion dryer, and an Interagency Monitoring of Protected Visual Environments
299 (IMPROVE; <https://vista.cira.colostate.edu/Improve/improve-program/>) aerosol sampler operated
300 at 22.8 L/min (Ruthenburg et al., 2014; Solomon et al., 2014). The aerosol generator and sampler
301 was used to generate and collect the known mass of each target compound onto 25 mm Teflon
302 filters (MTL, USA). De-ionized water (~18.2 M Ω purity) was used to make solutions of each
303 compound, for collecting blank filter samples in the aerosol generator and sampler system and to
304 flush the system. —Pure filtered air and chemical solutions were delivered to the atomizer to
305 generate aerosol particles. Before collecting each compound, a 30-minute pre-flush with water was
306 conducted to eliminate any residual material from the previous sample collection run.
307 Subsequently, a water blank was collected onto the Teflon filter to identify any remaining
308 contamination from prior samples. If contamination was identified, further cleaning was
309 performed. Following this, each compound was collected on a Teflon filter using an IMPROVE

310 aerosol sampler with sufficient mass (more than 50 μg , based on observations of sodium chloride's
 311 water uptake, as discussed in section 3.3) to produce measurable water uptake in the sample above
 312 its deliquescence RH (Table 1). After completing these steps, the aerosol generator and sampler
 313 underwent a 30-minute water flush to remove any deposited compounds, ensuring they were
 314 contamination-free for subsequent runs~~leaving it was contamination-free for subsequent runs.~~
 315 Following sample collection on the aerosol generator and sampler and prior to post-weighing, the
 316 collected samples were placed in a dry desiccator for a minimum of 24 hours to remove any
 317 residual water. Pre-weights and post-weights of filters were recorded at least thrice on three
 318 separate days using a high-precision ultra-microbalance with a readability of 0.1 μg (model XP2U,
 319 Mettler–Toledo, USA) before and after sample collection. ~~Following sample collection on the~~
 320 ~~aerosol generator and sampler and prior to post-weighing, the collected samples were placed in a~~
 321 ~~dry desiccator for a minimum of 24 hours to remove any residual water.~~ The difference in the post-
 322 weight and pre-weight gives the amount of compound collected on the filter.

323
 324 **Table 1.** List of compounds collected using aerosol generator and sampler for water uptake
 325 measurements

Compound	Chemical Formula	Molecular Weight (g/mol)	Density (g/cc)	Deliquescence Relative Humidity (DRH) (%) ^a
Ammonium Sulfate	(NH ₄) ₂ (SO ₄)	132.14	1.77	78 – 82
Sodium Chloride	NaCl	58.44	2.16	73 – 77
D-Glucose	C ₆ H ₁₂ O ₆	180.156	1.56	90 ^b
Malonic Acid	C ₃ H ₄ O ₄	104.0615	1.619	65 – 76

^aPeng et al., 2022; ^bMochida & Kawamura (2004)

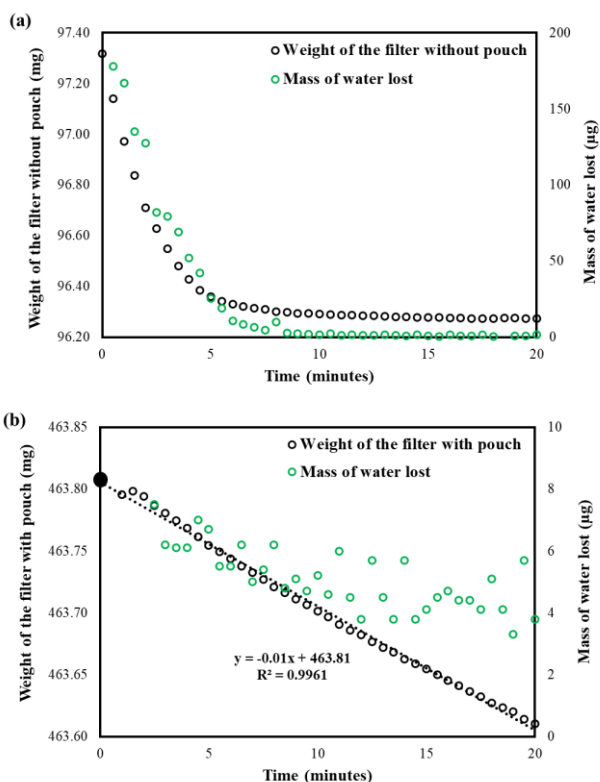
326 327 2.3. Water Uptake Measurements

328 After post-weighing, the dry particle-loaded filters (DS, post weighed filters with dry
 329 particles) were placed in sealed chambers at RHs of 84.3%, 90.8%, and 97.5%, and allowed to
 330 equilibrate for more than 24 hours. Subsequently, they were weighed to measure the water uptake
 331 by the solutes present on the filters. However, the weighing process did not proceed as expected;

332 the filter weights were unstable on the balance, gradually decreasing until they reached their initial
333 dry particle load weight (Fig. 2(a)). This indicated that the water taken up by compounds on the
334 filter was evaporating during the weighing process, making it impossible to measure the water
335 uptake at the chamber RH. Thus, there was a need for containment to prevent water loss during
336 weighing.

337 **2.3.1. How can we minimize water loss?**

338 To limit water loss during the wet weighing of the filter, different types of pouches were
339 used to contain the filter and lock in the humidity, including plastic and antistatic zip lock bags.
340 However, these proved to be ineffective due to electrostatic interference during weighing and
341 hygroscopicity of the pouch material. Consequently, aluminum foil pouches were tested. Pouches
342 (approximately 5 cm × 3 cm × 1 cm) were fabricated from these foils, with three sides sealed. The
343 weights of these pouches were quite stable; therefore, they were tested further for possible use in
344 the water uptake measurements.



345

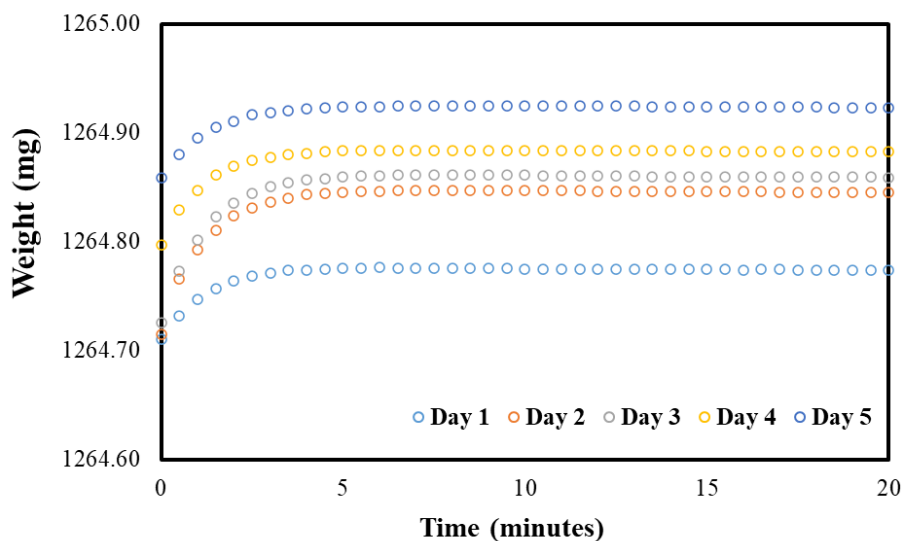
346 **Figure 2.** Weight of the filter and mass of water lost while weighing glucose ~~from~~at 97.5% RH:
 347 (a) without a pouch and (b) with a pouch. The dashed line represents the linear extrapolation of
 348 the observed filter weights to determine the actual wet filter weight (solid black circle) at the
 349 time the sample was taken from the chamber.

350 A dry particle-loaded filter was placed in a pouch and then placed in the chambers at the
 351 specified RH for more than 24 hours, with the fourth side open to allow water vapor in the air to
 352 interact with the particles on the filter. After equilibration and upon opening the chamber lid, the
 353 pouches were sealed immediately, and the time was recorded. Subsequently, the samples were
 354 transferred to the balance, and gravimetric readings were taken. The weight of the wet loaded
 355 sample (WSP, mass of the pouch with solute sample at measured RH) was recorded every 30
 356 seconds for 20 minutes (Fig 2b) to investigate how the wet weight of the filter with the pouch
 357 varied compared to that of the wet loaded filter without a pouch. The time taken for the sample
 358 transfer from the chamber to the first weight was also recorded.

359 Using a pouch to contain water loss while weighing proved to be effective. We observed a
360 small, slow decrease that achieved steady-state (noisy due to being close to the uncertainty of the
361 balance) after about 10 minutes in the wet weight of particulate filter with the pouch (fig 2(b)),
362 compared to the large, rapid decrease without the pouch (fig. 2(a)). The initial increase in mass,
363 followed by a linear decline required that the data be extrapolated from the linear region back to
364 time zero to accurately determine the net water uptake by the solute on the filter (fig. 2(b), dotted
365 line). These observations clearly suggest that the water loss from the filter can be nearly contained
366 by using the pouch. -Gold-coated aluminum foils were also tested and functioned similarly to
367 regular aluminum foil (Fig. S2). Gold-coated foils were used in subsequent experiments because
368 they come in separate sheets, making them easier to handle than rolled aluminum foil.

369 **2.3.2. Why does the pouch weight initially increase and then decrease?**

370 The initial weight gain of the pouch was perplexing, so we investigated by collecting wet
371 weight of a pouch with a filter and pouch without a filter (Figure 3) every 30 seconds for over 20
372 minutes. The same interval and duration of weighing were applied for all filters and tests unless
373 stated otherwise. This procedure was repeated for five days. -The weight increase in the initial
374 minutes of weighing was calculated using the measured data shown in Figure 3 and compared it
375 to the calculated change in air mass between wet and dry air using the psychometric data to
376 determine if dry air intrusion into the pouch was the cause of the weight gain.



377

378 **Figure 3.** Variation in the weight of the pouch with a Teflon filter over time starting when the
 379 pouch is removed from the chamber (RH = 97.5%) and placed on the balance.

380 **2.3.2.1. Measurements**

381 The observed variation in the weight of the pouch (with a filter) over time during the
 382 transition from measured RHs to the weighing balance, set at room RH, is depicted in Fig. 3.
 383 Across all days and with or without a filter, the weight variation followed a similar pattern,
 384 increasing for the first few minutes and then stabilizing.

385 The change in air mass for each day was determined by calculating the weight difference
 386 between the initial time and the point at which the weighing reached a near-constant, as illustrated
 387 in Eq. (62).

388
$$m_i = m_z - m_0 \tag{62}$$

389 where, m_z is the weight of pouch at time 'z' where it becomes constant, and m_0 is the weight of
 390 pouch at zero time.

391 The average (\pm SD) increases in mass from zero time to the point where the pouch (with a
 392 filter) weight became relatively constant for 84.3%, 90.8%, and 97.5% RHs was 95 (\pm 9) μ g, 98
 393 (\pm 56) μ g, and 97 (\pm 34) μ g, respectively.

394 2.3.2.2. Theoretical calculations using the Psychrometric Chart

395 The measured mass change was then compared to the calculated change in the mass of air
396 from the chamber RHs to room RH from the specific volume (SV) using the psychrometric chart
397 (PC) (source: https://daytonashrae.org/psychrometrics/psychrometrics_si.html#start) at the known
398 values of temperature and RHs. The assumption was made that the air inside the pouch was
399 exchanged for room air within a few minutes. During this time, an increase in weight would be
400 observed due to the displacement of less dense air (i.e. 97.5% RH) with denser air (~45% RH).
401 The obtained SV from the PC was then inverted to determine the density (ρ) of air at the respective
402 RHs, as shown in Eq. (23) & (34),

$$403 \rho_r = \frac{1}{SV_r} \quad (23)$$

$$405 \rho_i = \frac{1}{SV_i} \quad (34)$$

406
407 where, ρ_i represents the air density at different RHs (i : 84.3%, 90.8%, and 97.5%), and SV_i is the
408 specific volume at these RHs. ρ_r and SV_r represents the density and specific volume at room
409 conditions (r).

410 The net change in air density ($\Delta\rho$) from the measured relative humidities to room
411 conditions is calculated using the Eq. (45),

$$412 \Delta\rho = \rho_r - \rho_i \quad (45)$$

413 The variation in the mass of air (m_i) is calculated using the Eq. (56),

$$414 m_i = \Delta\rho \times V_p \quad (56)$$

415 where, m_i is the change in the mass of air from the measured RHs (84.3%, 90.8%, and 97.5%) to
416 the room RH and V_p is the volume of the aluminum pouch.

417 The calculated air density and mass obtained at high and room RHs using PC are presented
418 in Table S1. At higher RHs, the density of air in the pouch was lower, due to the increased
419 concentration of water molecules at higher RHs, which have a lower molecular weight (18 g/mol)
420 compared to that of air (29 g/mol). The calculated average net mass gain (\pm SD) from high RHs of

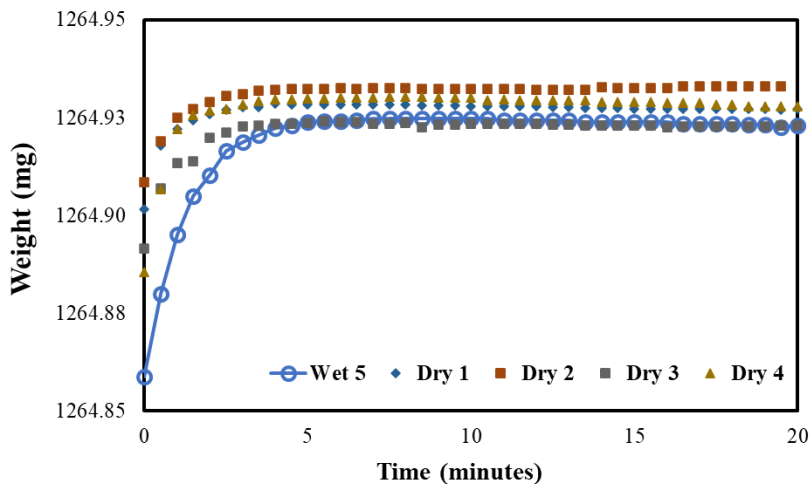
421 84.3%, 90.8%, and 97.5% to room RHs) was 197 (± 58) μg , 200 (± 52) μg , and 255 (± 54) μg ,
422 respectively.

423 The theoretical increase in the mass of air was higher than the measured values. This is
424 attributed to the air in the pouch being at a lower RH than the chamber RH at the initial weight
425 due to the time it takes to move the pouch from the glass chambers to the balance and an incomplete
426 exchange of high RH to room RH air.

427 **2.3.3. Increasing weights of filter with pouch during repeated measurements over multiple** 428 **days**

429 While conducting water uptake measurements, we observed that the weight of the pouch
430 with sampled filter was increasing from measurement to measurement even though the RH was
431 not changing, leading to uncertainty in our water uptake measurements (Fig. 3). There was a
432 consistent increase in the wet weight of the pouch with a filter for each consecutive day across all
433 RHs (84.3%, 90.8%, and 97.5%), with average ($\pm\text{SD}$) increases of 13 (± 10) μg , 17 (± 9) μg , and
434 37 (± 25) μg , respectively, as shown in Fig. 3 for 97.5% RH; results for 84.3% and 90.8% RH are
435 shown in Figure S3. Similarly, for the pouch without a filter, there was increases in weight of 14
436 (± 4) μg , 25 (± 11) μg , and 44 (± 7) μg , respectively (see Fig. S4).

437 To determine the cause of the mass increase, the following experiment was performed.
438 After conducting water uptake measurements for five days, the pouches with blank filters were
439 subsequently placed in a dry desiccator for a minimum of 24 hours and then weighed. This process
440 was repeated for the next four days. The observed variations in the weights of the dried pouches
441 are presented in Fig. 4 for 97.5% RH, and in Fig S3 for 84.3% and 90.8% RH. The weights of
442 these pouches, measured across all RHs, remained fairly consistent, only varying by a few
443 micrograms throughout the four days of measurement and did not exhibit a consistent trend in
444 either increasing or decreasing weight. This suggests that after water adsorption onto the pouch,
445 aluminum oxides are formed and remain stable at low RH. Considering these observations, it is
446 prudent to account for water adsorption onto pouches when making water uptake measurements.



447

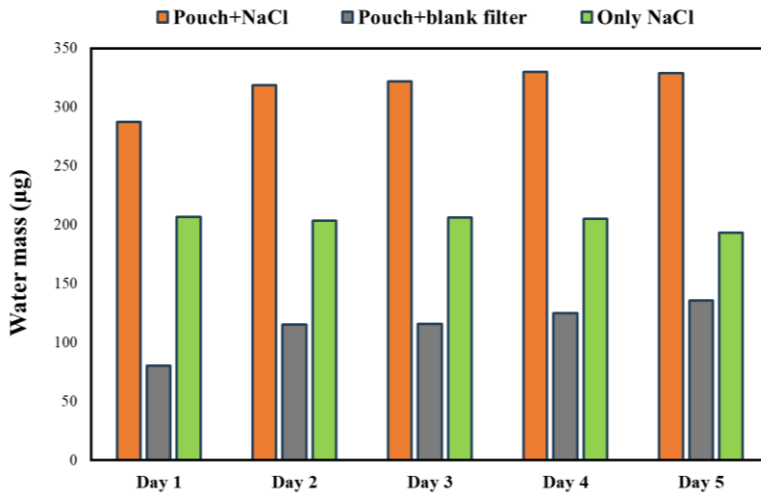
448 **Figure 4.** Variation in the dry weight of the pouch (with a filter) over time compared to the 5th
 449 day wet measurement (97.5% RH)

450

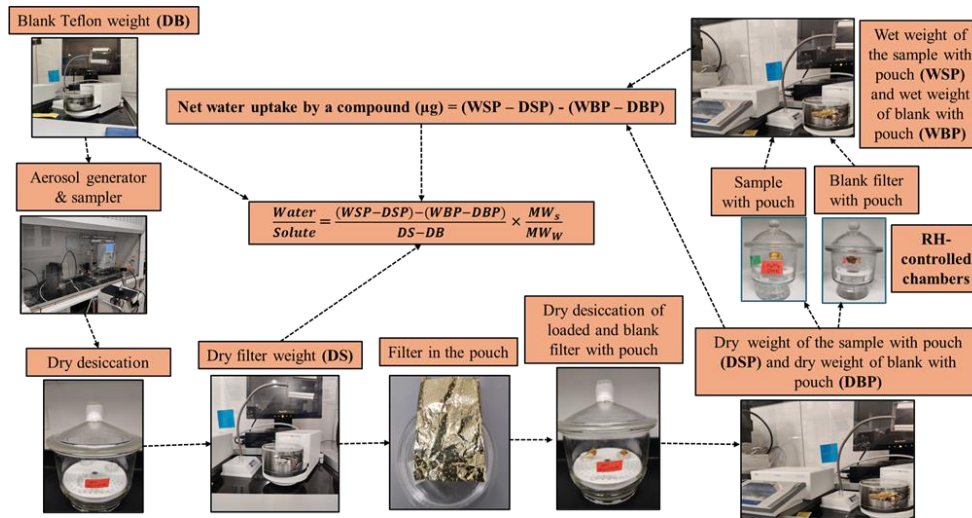
451 By including a measurement blank, consisting of a pouch with a blank filter, alongside the
 452 water uptake measurements using a pouch with a loaded filter, two issues are addressed: (i) water
 453 absorption on the pouch itself and (ii) small day to day fluctuations in the balance due to changes
 454 in meteorological and room conditions. The benefits of the measurement blank to account for water
 455 absorption on the pouch are illustrated with a filter loaded with sodium chloride and exposed to
 456 84.3% RH for five days. Figure 5 illustrates the water uptake of sodium chloride with the pouch,
 457 the pouch with blank filter, and the net water uptake by sodium chloride, calculated as the
 458 difference between the water uptake of the pouch with sodium chloride and the pouch with blank
 459 filter. The water uptake of the pouch with sodium chloride filter increased day to day. However,
 460 by subtracting the water uptake from the pouch with blank filter, the water uptake by sodium
 461 chloride remained consistent day to day. Hence, to address pouch absorption, measurements were
 462 conducted simultaneously on pouches with blank filters at the specified RHs and on pouches with
 463 loaded filters; thus, for each compound, there were a total of six filters—three pouches with blanks,
 464 one at 84.3%, 90.8%, and 97.5%, and similarly, three loaded filters in pouches at the same RH.

465 Figure 6 illustrates finalized water uptake methodology derived from the laboratory experiments
 466 conducted in this study.

Formatted: Indent: First line: 0"



467
 468 **Figure 5.** Water uptake by pouch with sodium chloride, pouch with blank filter, and only sodium
 469 chloride at 84.3% RH
 470



473
474 **Figure 6. Water uptake methodology developed in this study**

475 **2.4. Hygroscopic parameters estimation**

476 Four parameters related to hygroscopicity are reported here: mass fraction of solute (mfs),
477 molality, growth factor (GF), ~~and~~ the water-to-solute ratio, which is the number of moles of water
478 absorbed per mole of solute (compound). The calculations for these parameters are explained in
479 the following sections.

480 **2.4.1. Mass fraction of solute (mfs)**

481 The solute mass fraction is the fraction of solute relative to the total mass of the solution.
482 The mass of solution in the case of hygroscopic particles is the sum of solute's mass and the mass
483 of water absorbed by the solute at a given RH, as illustrated in Eq. (77):

484
$$\text{mfs} = \frac{\text{mass of solute } (\mu\text{g})}{\text{mass of solute } (\mu\text{g}) + \text{mass of water uptaken by the solute } (\mu\text{g})} \quad (77)$$

485
486
487 **2.4.2. Molality (m)**

488 Molality is the moles of solute dissolved in a certain mass of water, as illustrated in Eq.
489 (88):

490
$$\text{Molality (m, mol/kg)} = \frac{\text{no. of moles of solute}}{\text{mass of solvent (water absorbd by the solute)}} \quad (88)$$

491 **2.4.3. Growth Factor**

492 The growth factor (GF) of the dry particles at the measured RHs is estimated from the ratio
493 of wet particle diameter to the dry particle diameter, as shown in Eq. (99):

494
$$\text{GF}_j = \frac{D_{w,j}}{D_{dry}} \quad (99)$$

495 where, $D_{w,j}$ is the diameter of the wet particle at RH, j and D_{dry} is the diameter of dry particle. The
496 detailed calculations of GF at the respective RH are explained in Eq. (101) to Eq. (144):

497 Volume of the dry solute, $V_{\text{dry}} = \frac{\text{mass of solute}}{\text{density of solute}}$ (1010)

498 Volume of adsorbed water onto the solute, $V_{\text{water}} = \frac{\text{mass of water}}{\text{density of water}}$ (111)

499 Total volume of the wet particle, $V_{\text{wet}} = V_{\text{dry}} + V_{\text{water}}$ (122)

500 Average diameter of the wet particle, $D_{\text{wet}} = 2 \times \left(\frac{3V_{\text{wet}}}{4\pi}\right)^{\frac{1}{3}}$ (133)

501 Average diameter of the dry particle, $D_{\text{dry}} = 2 \times \left(\frac{3V_{\text{dry}}}{4\pi}\right)^{\frac{1}{3}}$ (144)

502 **2.4.4. Water-to-solute ratio**

503 Equation 155 gives the water/solute (W/S) of the sample on the filter in terms of the
504 measured quantities:

505
$$\frac{\text{Water}}{\text{Solute}} = \frac{(\text{wet sample with pouch} - \text{dry sample with pouch}) - (\text{wet blank with pouch} - \text{dry blank with pouch})}{\text{dry sample} - \text{dry blank}} \times \frac{MW_s}{MW_w}$$
 (155)

507 where, wet sample with pouch (WSP) is the mass of the pouch and sampled filter at high RH, dry
508 sample with pouch (DSP) is the mass of the pouch with particles on the filter at dry conditions,
509 wet blank with pouch (WBP) is the mass of the pouch with blank filter at high RH, dry blank with
510 pouch (DBP) is the mass of the pouch with blank filter at dry conditions, dry sample (DS) is the
511 mass of the filter with particles on the filter at dry condition, and dry blank (DB) is the mass of the
512 blank filter. MW_s and MW_w are the molecular weight of solute and water, respectively. All are in
513 the units of milligrams (mg), except MW, ~~mol/gmmol~~.

514 **2.5. Uncertainty in the measured water-to-solute (W/S) ratio**

515 The uncertainty of the measured water-to-solute ratio was determined using the partial
516 derivatives of the input parameters employed in calculating the W/S ratio.

517 From Eq. (155), the W/S ratio can be written as

518
$$\frac{W}{S} = \frac{(WSP - DSP) - (WBP - DBP)}{DS - DB} \times \frac{MW_s}{MW_w}$$
 (166)

519 The sensitivity of the W/S ratio to the input variables (X) were calculated using partial derivatives

520 $(\frac{\partial(W/S)}{\partial(X)})$, as illustrated in Eq. (177) through (222):

521 $|\frac{\partial(W/S)}{\partial(WSP)}| = |\frac{1}{DS-DB}|$ (177)

522 $|\frac{\partial(W/S)}{\partial(DSP)}| = |\frac{1}{DB-DS}|$ (188)

523 $|\frac{\partial(W/S)}{\partial(WBP)}| = |\frac{1}{DB-DS}|$ (199)

524 $|\frac{\partial(W/S)}{\partial(DBP)}| = |\frac{1}{DS-DB}|$ (2020)

525 $|\frac{\partial(W/S)}{\partial(DS)}| = |\frac{-(WSP-DSP)+(WBP-DBP)}{(DS-DB)^2}|$ (211)

526 $|\frac{\partial(W/S)}{\partial(DB)}| = |\frac{(WSP-DSP)-(WBP-DBP)}{(DS-DB)^2}|$ (222)

527 The uncertainty contribution δX of each input variable (X) to the measured W/S ratio was

528 estimated using Eq. (233):

529 $\delta X = |\frac{\partial(W/S)}{\partial X}| \times \sigma(X)$ (233)

530 where, $\sigma(X)$ is the standard deviation of each input parameter (X).

531 The overall uncertainty in the measured W/S was calculated using Eq. (244):

532 $\delta(W/S) = \sum(|\frac{\partial(W/S)}{\partial(X)}| \times \sigma(X))$ (244)

533 The percentage uncertainty contribution by each input variable to total uncertainty in the W/S ratio

534 was calculated using Eq. (255):

535 $\frac{\delta(X)}{W/S} \times 100$ (255)

536 3. Results and Discussion

537 3.1. Derived hygroscopic parameters

538 Table 2 shows the hygroscopic parameters derived from the measurements, including
539 water-to-solute (W/S) ratio, mfs, molality, and GF at the measured RHs for ammonium sulfate,

540 sodium chloride, glucose, and malonic acid. The observed water uptake increased from 84.3% to
 541 97.5% RH for all compounds. For example, the observed W/S ratio of sodium chloride i.e. moles
 542 of water absorbed per mole of sodium chloride was 14.62 at 84.3% RH, 19.8 at 90.8% RH and 86
 543 at 97.5% RH. Similarly, for ammonium sulfate, glucose, and malonic acid, the W/S increased from
 544 an RH of 84.3% to 97.5% by factors of 5.0, 4.8, and 6.9, respectively. Conversely, the mfs and
 545 molality decreased with increasing RH for all the measured compounds. For example, the mfs of
 546 malonic acid was 0.47 at 84.3% RH, but only 0.11 at 97.5% RH. Similarly, the observed molality
 547 for malonic acid was 8.63 at 84.3% RH, which reduced to 1.25 at 97.5% RH.

548
549
550
551
552
553
554
555

556 **Table 2.** Derived hygroscopic parameters from this study's developed methodology (n = 5)

	RH=84.3%		RH=90.8%		RH=97.5%	
	Mean	SD	Mean	SD	Mean	SD
Ammonium sulfate						
W/S	9.26	0.71	16.9	1.24	45.69	0.43
MFS	0.44	0.02	0.3	0.02	0.14	0.00
Molality	6.03	0.48	3.3	0.26	1.22	0.01
GF	1.47	0.03	1.7	0.04	2.29	0.01
Sodium chloride						
W/S	14.62	0.40	19.80	0.32	85.98	2.53
MFS	0.18	0	0.14	0	0.04	0
Molality	3.80	0.11	2.80	0.05	0.65	0.02
GF	2.23	0.003	2.45	0.02	3.88	0.04
Glucose						
W/S	6.82	0.17	9.62	0.94	33.09	1.40
MFS	0.59	0.01	0.51	0.02	0.23	0.01

Molality	8.14	0.21	5.81	0.57	1.68	0.07
GF	1.29	0.01	1.36	0.03	1.83	0.02
Malonic acid						
W/S	6.45	0.27	10.93	0.55	44.69	3.39
MFS	0.47	0.01	0.35	0.01	0.11	0.01
Molality	8.63	0.35	5.09	0.26	1.25	0.09
GF	1.27	0.01	1.6	0.02	2.38	0.05

557

558 In this study, the water uptake measurements for each compound at each specific RH were
559 repeated over five different days to investigate the repeatability of the determined hygroscopic
560 parameters. The variability (standard deviation) in the observed hygroscopic parameters, as shown
561 in Table 2, is small. For instance, the relative standard deviation (RSD, $SD \div \text{mean}$) of the growth
562 factor for malonic acid at all RHs was less than 0.5%. This observation clearly indicates that the
563 variability of measured hygroscopic parameters at the same RH for each compound between
564 different experiment days is minimal, highlighting the repeatability of this methodology. In
565 addition, to examine the reproducibility of this methodology, we repeated the water uptake
566 measurement for the malonic acid compound at 97.5% RH with different masses (48.8 μg and
567 130.4 μg) and estimated the hygroscopic parameters. We observed insignificant differences
568 ($\sim 0.4\%$) in the water uptake parameters of malonic acid at 97.5% RH between the two experiments.
569 These observations indicate that the developed methodology can reproducibly assess the
570 hygroscopicity of particles collected on Teflon filters.

571 In our study, we recorded the wet weight every 30 seconds over 20 minutes to estimate the
572 hygroscopic parameters. However, we evaluated if this length of time was necessary by calculating
573 the GFs for each compound at the measured RHs for 5, 10, and 15-minute intervals and compared
574 them with the GFs using the 20-minute interval, shown in Figure S5. There was no significant
575 difference between the GFs estimated using the 5, 10, 15 and 20-minute intervals. For future
576 studies, it is unnecessary to take wet weighing for 20 minutes; and taking wet weights every 30
577 seconds over a 5-minute period is sufficient to determine hygroscopic parameters.

578 3.2. Comparison of estimated hygroscopic parameters with previous studies

579 Most of the prior studies reported the water uptake in terms of GFs with few reported in terms of
580 mfs and molality so we will focus our comparisons on GF measurements. The estimated average
581 GFs for each compound at the measured RHs were compared with previous studies, depicted in

582 Fig. 76. -These studies used techniques such as HTDMA and EDB to derive GF. These studies
583 typically examined RH levels of 90% or lower, except for Mikhailov et al., (2024), who estimated
584 GFs for ammonium sulfate and glucose at RH levels up to 99.9%. Additionally, the estimated GFs
585 for compounds were compared with values provided by the thermodynamic model, E-AIM
586 (<http://www.aim.env.uea.ac.uk/aim/aim.php>), which has been widely used to assess the water
587 uptake of inorganic compounds for over three decades. The estimated GF for sodium chloride of
588 2.23 at 84.3% RH was similar to values reported in previous studies (M. Cheng & Kuwata, 2023;
589 Hu et al., 2010; Peng et al., 2016), which ranged from 2–2.22. Similarly, at 90.8% RH, the
590 observed GF for sodium chloride of 2.45 was close to previous findings (M. Cheng & Kuwata,
591 2023; Peng et al., 2016; Zieger et al., 2017), which ranged from 2.20–2.40. For ammonium sulfate,
592 the observed GFs at 84.3%, 90.8, and 97.5% RH were 1.47, 1.7, 2.29, respectively, which are
593 similar to those of previous studies (Bouzidi et al., 2020; M. Cheng & Kuwata, 2023; Choi &
594 Chan, 2002; Cruz & Pandis, 2000; Denjean et al., 2014; Hämeri et al., 2002; Hu et al., 2010;
595 Koehler et al., 2006; Liu et al., 2016; Mikhailov et al., 2024; Prenni et al., 2001; Sjogren et al.,
596 2007), which were 1.49–1.60, 1.70–1.79, and 2.3, respectively. Likewise, for glucose, at 84.3%,
597 90.8%, and 97.5% RH, the observed GFs fell within the ranges reported in earlier studies (Lei et
598 al., 2023; Mikhailov et al., 2024; Mochida & Kawamura, 2004), which were 1.2–1.5, 1.3–1.65,
599 and 1.8 respectively. For malonic acid, the observed GFs at 84.3% and 90.8% RH were consistent
600 with the ranges found in previous studies (Bouzidi et al., 2020; Peng et al., 2001; Pope et al., 2010;
601 Prenni et al., 2001). The measured GF for ammonium sulfate and sodium chloride at all RH levels
602 agreed well with the E-AIM model values, except at 97.5% RH. The observed GF for ammonium
603 sulfate at 97.5% in this study was slightly lower than the value reported by E-AIM, differing by a
604 factor of 1.11. For sodium chloride, it was higher by a factor of 1.12. Changes in water uptake near
605 saturation RH are steep, and even slight variations in RH can significantly affect the GF. This
606 likely explains the slight differences between this study and the E-AIM at 97.5% RH.

607 This study's observed average mfs of malonic acid for 84.3%, 90.8%, and 97.5% RH was
608 0.47, 0.35, and 0.11, respectively, which are similar to those of previous studies (0.475, 0.37–0.38,
609 and 0.11, respectively) as reported by Koehler et al. (2006) and Maffia & Meirelles (2001). In the
610 same way, for other compounds, the observed mfs are closely matched with those of previous
611 studies (ammonium sulfate: 0.37–0.42, 0.3–0.32, and 0.1–0.12 (Chan et al., 1992; Kim et al., 1994;
612 Kreidenweis et al., 2005; Mikhailov et al., 2024); glucose: 0.60, 0.44–0.46, 0.25 (Mikhailov et al.,

613 2024; Peng et al., 2001); sodium chloride: 0.175, 0.04 (Kreidenweis et al., 2005)). Few studies
614 have reported water uptake in terms of molality, and the observed molality for all the compounds
615 in this study were close to the range of those reported in previous studies (Ammonium sulfate: ~4–
616 6.5, 3–3.2, and 1 (Y. Cheng et al., 2015; Mikhailov et al., 2024; Zamora & Jacobson, 2013),
617 Glucose: ~5.25–8, 4.7, and 1 (Lei et al., 2023; Mikhailov et al., 2024; Zamora et al., 2011), Malonic
618 acid: ~8.5, 5.7, and 1.25 (Lee & Hildemann, 2013)), and sodium chloride: ~4.25, 2.2, and 0.75
619 (Zamora & Jacobson, 2013)).

620

621

622

623

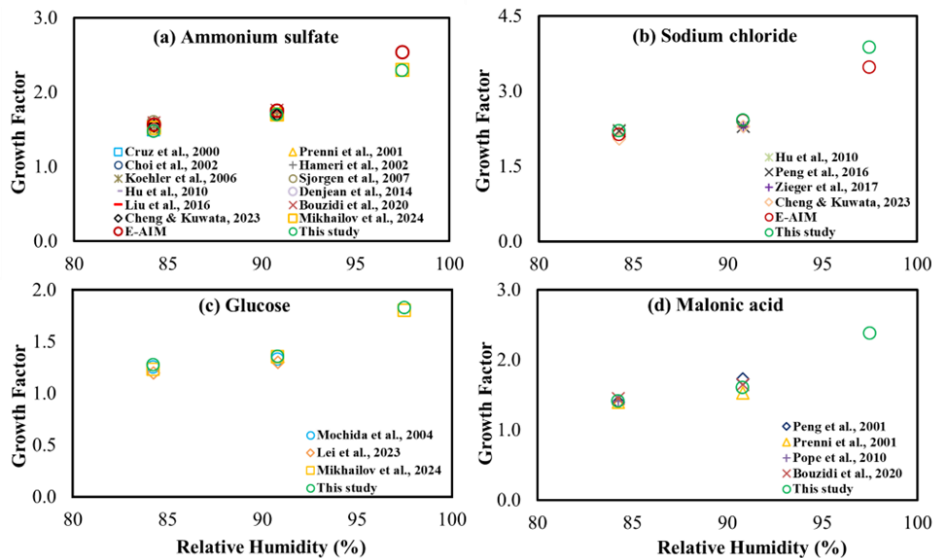
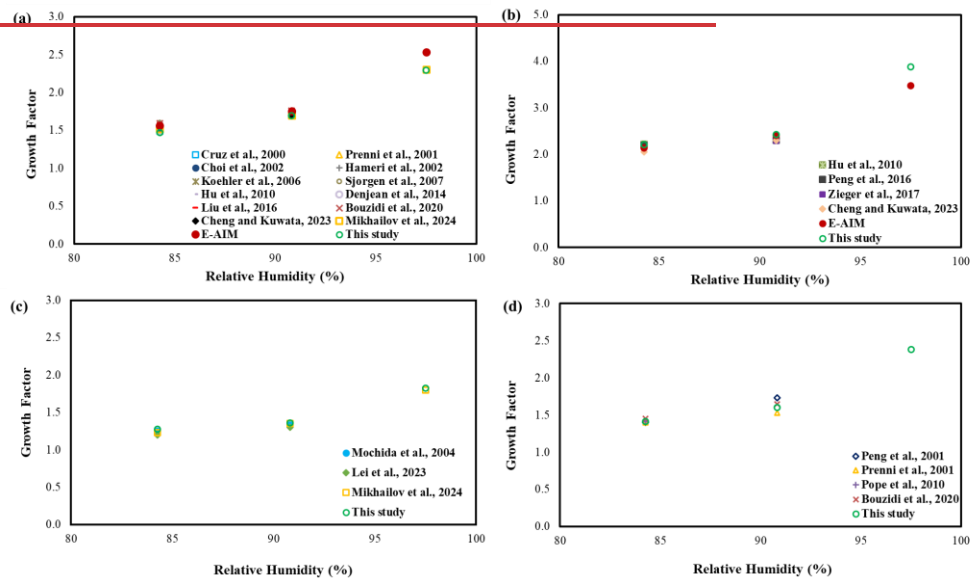


Figure 7. Comparison of estimated growth factor for (a) Ammonium sulfate, (b) Sodium chloride, (c) Glucose, and (d) Malonic acid with previous studies

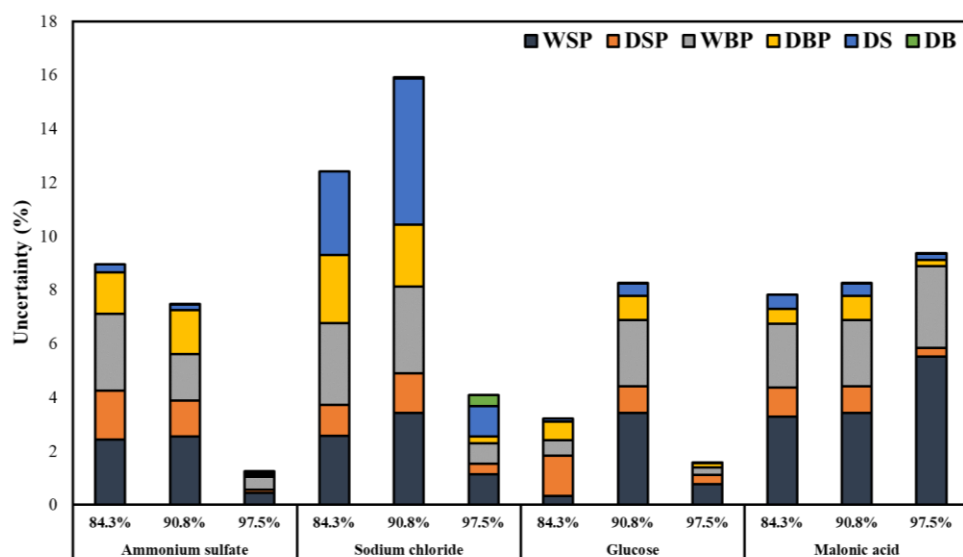


628 ~~Figure 6. Comparison of estimated growth factor for (a) Ammonium sulfate, (b) sodium~~
629 ~~chloride, (c) Glucose, and (d) Malonic acid with previous studies~~

630
631 The above comparisons validates the accuracy and reliability of the methodology used in
632 this study. Therefore, the water uptake of particles collected on Teflon filters can be effectively
633 assessed using the developed methodology.

634 3.3. Estimated uncertainties in the W/S ratio

635 The estimated uncertainties in the W/S ratio using this study's methodology are depicted
636 in Fig. ~~87~~. Overall, the uncertainty for almost all the measured compounds at measured RHs was
637 below 10%, except for sodium chloride at 84.3% and 90.8%, which had uncertainties of 12% and
638 15%, respectively. WSP and WBP contributed the most to the overall W/S uncertainty, followed
639 by DSP and DBP, with DS and DB contributing the least for all the measured compounds, except
640 sodium chloride. For sodium chloride, consistent water uptake was observed across all five
641 measured days, as exemplified by the net water uptake at 84% RH, shown in Fig. 5. However, for
642 sodium chloride, the major uncertainty was associated with DS, unlike other compounds. A
643 plausible reason for this discrepancy is the smaller mass of sodium chloride (45, 39.5, and 27.8 μg
644 for 84.3, 90.8, and 97.5% RHs, respectively) compared to other compounds which averaged 122,
645 274 and 88 μg for ammonium sulfate, glucose, and malonic acid, respectively for all three RHs
646 ~~The lower mass increases uncertainty due to the limitations in the precision of the balance.~~ For
647 sodium chloride at 97.5%, water uptake was more than 3 times higher than at 84.3 and 90.8% RH
648 resulting in lower uncertainty at 97.5%. This discrepancy is inherent in the W/S ratio calculation,
649 as the mass of solute is in the denominator. Nevertheless, it is important to note that this uncertainty
650 is not inherent in the developed methodology but rather caused by the lower mass used for sodium
651 chloride in the water uptake measurements. To reduce this uncertainty, based on our observations,
652 we recommend using a larger mass: at least 50 μg for hygroscopic compounds like sodium
653 chloride, 100 μg for medium hygroscopic compounds like glucose, and more than 200 μg for less
654 hygroscopic compounds.



656
657 **Figure 78.** Estimated uncertainties in the measured water-to-solute ratio at different RHs.
658
659

660
661 **4. Conclusion**

662 In this study, we developed a novel methodology to assess the water uptake of particulate
663 samples collected on Teflon filters. By using filter samples, the chemical composition of ambient
664 or chamber samples can be measured as well as water uptake, something neither HTDMA nor
665 EDB can do for complex mixtures. The advantage of this method is that it enables hygroscopicity
666 to be related to chemical composition. Additionally, this method can be used to measure water uptake
667 above 90% RH, which is typically not done with HTDMA measurements.

668 Laboratory hygroscopic measurements were conducted for ammonium sulfate, sodium
669 chloride, glucose, and malonic acid. Constant humidity solutions were employed to maintain
670 specific RH and enable measurements as high as ~97%. While conducting water uptake
671 measurements, we encountered problems, including water loss from the filter when moving from

Formatted: Indent: First line: 0.5"

672 high RH to room RH for weighing, and absorption by the pouch used to contain the water loss
673 from the filter sample. These problems were successfully addressed by placing the sample filter in
674 an aluminum pouch and accounting for water absorption by the pouch itself. Constant humidity
675 solutions were employed to maintain specific RH and enable measurements as high as 97%.
676 Hygroscopic parameters, including the W/S ratio, GF, molality, and the mfs, were estimated from
677 water uptake measurements for ammonium sulfate, sodium chloride, glucose, and malonic acid at
678 RH levels of 84.3%, 90.8%, and 97.5%. As expected, the water uptake increased with higher RH
679 for all compounds. The observed GFs in this study were consistent with those reported in previous
680 studies for all the measured compounds at the examined RH levels, and similar to modelled values
681 for the inorganics highlighting the accuracy of this method. The overall uncertainty in the observed
682 W/S ratio was less than 10% for most of the compound/RH combinations measured, further
683 highlighting robustness and precision of this new method.

684 The method developed in this study can be used to measure water uptake on the same
685 samples used to measure chemical composition for ambient, indoor and chamber studies. For
686 organic aerosol composition, Fourier-transform infrared spectroscopy (FT-IR), which is not
687 destructive to the filter sample, can be used to quantify the organic carbon and organic functional
688 groups present in the particles collected on Teflon filters (Anunciado et al., 2023; Boris et al.,
689 2019; Debus et al., 2022; Li et al., 2024; Yazdani et al., 2021). Other non-destructive methods
690 such as gravimetry for total mass, light absorption measurements to estimate elemental carbon
691 (White et al., 2016) and X-ray fluorescence (XRF) to measure elements (Gorham et al., 2021;
692 Hyslop et al., 2015) provide additional composition information. After the water uptake
693 measurements are performed, the filter sample can be extracted to measure inorganic ions, sulfate,
694 nitrate and ammonium to complete the compositional measurements on the filter. Alternatively,
695 simultaneous sampling of multiple filters including a Teflon filter, such as is done for the
696 IMPROVE and the Chemical Speciation Network (Solomon et al., 2014) provide high quality
697 speciation data. This integrated approach ensures that the chemical analysis corresponds to the air
698 sample from which water uptake data is obtained. Furthermore, using modeled estimates of
699 inorganic water uptake, the measured water uptake can be apportioned between organic and
700 inorganic components.

701

Formatted: Indent: First line: 0.5"

702 **Author Contributions**

703 ASW and AMD conceived of the project. NR developed the water uptake methodology, performed
704 the laboratory work and data analysis, created the figures and tables, and wrote and edited the
705 manuscript. ASW and AMD provided leadership for the project, including mentoring and
706 supervising NR in the laboratory work, methodology development and data analysis, and reviewed
707 and edited the manuscript.

708 **Competing interests**

709 The contact author has declared that none of the authors has any competing interests.

710 **Acknowledgements**

711 We would like to thank the Department of Energy (DOE), USA, for funding this project (grant no.
712 DE-SC0023087). We also acknowledge the support of undergraduate students Lucas Wang and
713 Alexander Velasco in the laboratory measurements.

714 **References**

- 715 [Anunciado, M. B., De Boskey, M., Haines, L., Lindskog, K., Dombek, T., Takahama, S., &](#)
716 [Dillner, A. M. \(2023\). Stability assessment of organic sulfur and organosulfate compounds](#)
717 [in filter samples for quantification by Fourier- transform infrared spectroscopy.](#)
718 [Atmospheric Measurement Techniques, 16\(14\), 3515–3529. https://doi.org/10.5194/amt-](#)
719 [16-3515-2023](#)
- 720 Boreddy, S. K. R., Kawamura, K., & Jung, J. (2014). Hygroscopic properties of particles nebulized
721 from water extracts of aerosols collected at Chichijima Island in the western North Pacific:
722 An outflow region of Asian dust. *Journal of Geophysical Research: Atmospheres*, 119(1),
723 167–178. <https://doi.org/10.1002/2013JD020626>
- 724 Boris, A. J., Takahama, S., Weakley, A. T., Debus, B. M., Fredrickson, C. D., Esparza-Sanchez,
725 M., Burki, C., Reggente, M., Shaw, S. L., Edgerton, E. S., & Dillner, A. M. (2019).
726 Quantifying organic matter and functional groups in particulate matter filter samples from
727 the southeastern United States – Part 1: Methods. *Atmospheric Measurement Techniques*,
728 12(10), 5391–5415. <https://doi.org/10.5194/amt-12-5391-2019>

- 729 Bouzidi, H., Zuend, A., Ondráček, J., Schwarz, J., & Ždímal, V. (2020). Hygroscopic behavior of
730 inorganic–organic aerosol systems including ammonium sulfate, dicarboxylic acids, and
731 oligomer. *Atmospheric Environment*, 229, 117481.
732 <https://doi.org/10.1016/j.atmosenv.2020.117481>
- 733 Chan, C. K., Flagan, R. C., & Seinfeld, J. H. (1992). Water activities of $\text{NH}_4\text{NO}_3/(\text{NH}_4)_2\text{SO}_4$
734 solutions. *Atmospheric Environment. Part A. General Topics*, 26(9), 1661–1673.
735 [https://doi.org/10.1016/0960-1686\(92\)90065-S](https://doi.org/10.1016/0960-1686(92)90065-S)
- 736 Chan, C. K., Ha, Z., & Choi, M. Y. (2000). Study of water activities of aerosols of mixtures of
737 sodium and magnesium salts. *Atmospheric Environment*, 34(28), 4795–4803.
738 [https://doi.org/10.1016/S1352-2310\(00\)00252-1](https://doi.org/10.1016/S1352-2310(00)00252-1)
- 739 Cheng, M., & Kuwata, M. (2023). Development of the low-temperature hygroscopicity tandem
740 differential mobility analyzer (Low-T HTDMA) and its application to $(\text{NH}_4)_2\text{SO}_4$ and
741 NaCl particles. *Journal of Aerosol Science*, 168, 106111.
742 <https://doi.org/10.1016/j.jaerosci.2022.106111>
- 743 Cheng, Y., Su, H., Koop, T., Mikhailov, E., & Pöschl, U. (2015). Size dependence of phase
744 transitions in aerosol nanoparticles. *Nature Communications*, 6(1), 5923.
745 <https://doi.org/10.1038/ncomms6923>
- 746 Choi, M. Y., & Chan, C. K. (2002). The Effects of Organic Species on the Hygroscopic Behaviors
747 of Inorganic Aerosols. *Environmental Science & Technology*, 36(11), 2422–2428.
748 <https://doi.org/10.1021/es0113293>
- 749 Clegg, S. L., Brimblecombe, P., & Wexler, A. S. (1998). Thermodynamic Model of the System H^+
750 $-\text{NH}_4^+ - \text{SO}_4^{2-} - \text{NO}_3^- - \text{H}_2\text{O}$ at Tropospheric Temperatures. *The Journal of Physical*
751 *Chemistry A*, 102(12), 2137–2154. <https://doi.org/10.1021/jp973042r>
- 752 Cohen, M. D., Flagan, R. C., & Seinfeld, J. H. (1987). Studies of concentrated electrolyte solutions
753 using the electrodynamic balance. 1. Water activities for single-electrolyte solutions. *The*
754 *Journal of Physical Chemistry*, 91(17), 4563–4574. <https://doi.org/10.1021/j100301a029>
- 755 Cruz, C. N., & Pandis, S. N. (2000). Deliquescence and Hygroscopic Growth of Mixed
756 Inorganic–Organic Atmospheric Aerosol. *Environmental Science & Technology*, 34(20),
757 4313–4319. <https://doi.org/10.1021/es9907109>
- 758 Debus, B., Weakley, A. T., Takahama, S., George, K. M., Amiri-Farahani, A., Schichtel, B.,
759 Copeland, S., Wexler, A. S., & Dillner, A. M. (2022). Quantification of major particulate

Formatted: Line spacing: 1.5 lines

760 [matter species from a single filter type using infrared spectroscopy – application to a](#)
761 [large-scale monitoring network. *Atmospheric Measurement Techniques*, 15\(9\), 2685–](#)
762 [2702. https://doi.org/10.5194/amt-15-2685-2022](#)

764 Denjean, C., Formenti, P., Picquet-Varrault, B., Katrib, Y., Pangui, E., Zapf, P., & Doussin, J. F.
765 (2014). A new experimental approach to study the hygroscopic and optical properties of
766 aerosols: Application to ammonium sulfate particles. *Atmospheric Measurement*
767 *Techniques*, 7(1), 183–197. <https://doi.org/10.5194/amt-7-183-2014>

768 Fredenslund, A., Jones, R. L., & Prausnitz, J. M. (1975). Group-contribution estimation of activity
769 coefficients in nonideal liquid mixtures. *AIChE Journal*, 21(6), 1086–1099.
770 <https://doi.org/10.1002/aic.690210607>

771 Greenspan, L., (1976). Humidity Fixed Points of Binary Saturated Aqueous Solutions. Journal of
772 Research of the National Bureau of Standards - A. Physics and Chemistry, 81A, 1.

773 [Gorham, K. A., Raffuse, S. M., Hyslop, N. P., & White, W. H. \(2021\). Comparison of recent](#)
774 [speciated PM_{2.5} data from collocated CSN and IMPROVE measurements. *Atmospheric*](#)
775 [Environment, 244, 117977. https://doi.org/10.1016/j.atmosenv.2020.117977](#)

776 [Gu, W., Li, Y., Zhu, J., Jia, X., Lin, Q., Zhang, G., Ding, X., Song, W., Bi, X., Wang, X., & Tang,](#)
777 [M. \(2017\). Investigation of water adsorption and hygroscopicity of atmospherically](#)
778 [relevant particles using a commercial vapor sorption analyzer. *Atmospheric Measurement*](#)
779 [Techniques, 10\(10\), 3821–3832. https://doi.org/10.5194/amt-10-3821-2017](#)

781 Gupta, T., Rajeev, P., & Rajput, R. (2022). Emerging Major Role of Organic Aerosols in
782 Explaining the Occurrence, Frequency, and Magnitude of Haze and Fog Episodes during
783 Wintertime in the Indo Gangetic Plain. *ACS Omega*, 7(2), 1575–1584.
784 <https://doi.org/10.1021/acsomega.1c05467>

785 Hämeri, K., Charlson, R., & Hansson, H. (2002). Hygroscopic properties of mixed ammonium
786 sulfate and carboxylic acids particles. *AIChE Journal*, 48(6), 1309–1316.
787 <https://doi.org/10.1002/aic.690480617>

788 Han, S., Hong, J., Luo, Q., Xu, H., Tan, H., Wang, Q., Tao, J., Zhou, Y., Peng, L., He, Y., Shi, J.,
789 Ma, N., Cheng, Y., & Su, H. (2022). Hygroscopicity of organic compounds as a function

Formatted: Font: (Default) +Body (Aptos), 11 pt

Formatted: Normal, Left

Formatted: Line spacing: 1.5 lines

790 of organic functionality, water solubility, molecular weight, and oxidation level.
791 *Atmospheric Chemistry and Physics*, 22(6), 3985–4004. [https://doi.org/10.5194/acp-22-](https://doi.org/10.5194/acp-22-3985-2022)
792 3985-2022

793 Haseeb, M., Tahir, Z., Mahmood, S. A., Batool, S., Tariq, A., Lu, L., & Soufan, W. (2024). Spatio-
794 temporal assessment of aerosol and cloud properties using MODIS satellite data and a
795 HYSPLIT model: Implications for climate and agricultural systems. *Atmospheric*
796 *Environment: X*, 21, 100242. <https://doi.org/10.1016/j.aeaoa.2024.100242>

797 [Hitzenberger, R., Berner, A., Dusek, U., & Alabashi, R. \(1997\). Humidity-Dependent Growth of](#)
798 [Size-Segregated Aerosol Samples. *Aerosol Science and Technology*, 27\(2\), 116–130.](#)
799 <https://doi.org/10.1080/02786829708965461>

Formatted: Line spacing: 1.5 lines

800 ▲

Formatted: Font: (Default) +Body (Aptos), 11 pt

Formatted: Normal, Left

801 Hu, D., Qiao, L., Chen, J., Ye, X., Yang, X., Cheng, T., & Fang, W. (2010). Hygroscopicity of
802 Inorganic Aerosols: Size and Relative Humidity Effects on the Growth Factor. *Aerosol and*
803 *Air Quality Research*, 10(3), 255–264. <https://doi.org/10.4209/aaqr.2009.12.0076>

804 [Hyslop, N. P., Trzepla, K., & White, W. H. \(2015\). Assessing the Suitability of Historical PM_{2.5}](#)
805 [Element Measurements for Trend Analysis. *Environmental Science & Technology*,](#)
806 [49\(15\), 9247–9255. https://doi.org/10.1021/acs.est.5b01572](https://doi.org/10.1021/acs.est.5b01572)

Formatted: Line spacing: 1.5 lines

807 ▲

Formatted: Font: (Default) +Body (Aptos), 11 pt

Formatted: Normal, Left

808 Jathar, S. H., Mahmud, A., Barsanti, K. C., Asher, W. E., Pankow, J. F., & Kleeman, M. J. (2016).
809 Water uptake by organic aerosol and its influence on gas/particle partitioning of secondary
810 organic aerosol in the United States. *Atmospheric Environment*, 129, 142–154.
811 <https://doi.org/10.1016/j.atmosenv.2016.01.001>

812 [Jose, C., Singh, A., Kalkura, K. N., Jose, G. V., Srivastava, S., Ammini, R. K., Yadav, S.,](#)
813 [Ravikrishna, R., Andreae, M. O., Martin, S. T., Liu, P., & Gunthe, S. S. \(2024\). Complex](#)
814 [Hygroscopic Behavior of Ambient Aerosol Particles Revealed by a Piezoelectric](#)
815 [Technique. *ACS Earth and Space Chemistry*, 8\(5\), 983–991.](#)
816 <https://doi.org/10.1021/acsearthspacechem.3c00347>

Formatted: Line spacing: 1.5 lines

817 ▲

Formatted: Font: (Default) +Body (Aptos), 11 pt

Formatted: Normal, Left

- 818 Kohli, R.K., Davis, R. D., & Davies, J. F. (2023). Tutorial: Electrodynamic balance methods for
819 single particle levitation and the physicochemical analysis of aerosol. *Journal of Aerosol*
820 *Science*, 174, 106255. <https://doi.org/10.1016/j.jaerosci.2023.106255>
- 821 Kim, Y. P., Pun, B. K.-L., Chan, C. K., Flagan, R. C., & Seinfeld, J. H. (1994). Determination of
822 Water Activity in Ammonium Sulfate and Sulfuric Acid Mixtures Using Levitated Single
823 Particles. *Aerosol Science and Technology*, 20(3), 275–284.
824 <https://doi.org/10.1080/02786829408959683>
- 825 Kim, Y. P., & Seinfeld, J. H. (1995). Atmospheric Gas–Aerosol Equilibrium: III. Thermodynamics
826 of Crustal Elements Ca^{2+} , K^{+} , and Mg^{2+} . *Aerosol Science and Technology*, 22(1), 93–
827 110. <https://doi.org/10.1080/02786829408959730>
- 828 Koehler, K. A., Kreidenweis, S. M., DeMott, P. J., Prenni, A. J., Carrico, C. M., Ervens, B., &
829 Feingold, G. (2006). Water activity and activation diameters from hygroscopicity data –
830 Part II: Application to organic species. *Atmos. Chem. Phys.*
- 831 Kreidenweis, S. M., Koehler, K., DeMott, P. J., Prenni, A. J., Carrico, C., & Ervens, B. (2005).
832 Water activity and activation diameters from hygroscopicity data – Part I: Theory and
833 application to inorganic salts. *Atmos. Chem. Phys.*
- 834 [Kreidenweis, S. M. and Asa-Awuku, A.: 5.13 – Aerosol Hygroscopicity: Particle Water Content](#)
835 [and Its Role in Atmospheric Processes, in: Treatise on Geochemistry \(Second Edition\),](#)
836 [edited by: Turekian, K. K., Elsevier, Oxford, 331–361, 2014.](#)
- 837 ▲
- 838 Krumgalz, B.S. (2018). Temperature Dependence of Mineral Solubility in Water. Part 3.
839 Alkaline and Alkaline Earth Sulfates. *Journal of Physical and Chemical Reference Data*,
840 47, 023101.
- 841 Laskina, O., Morris, H. S., Grandquist, J. R., Qin, Z., Stone, E. A., Tivanski, A. V., & Grassian,
842 V. H. (2015). Size Matters in the Water Uptake and Hygroscopic Growth of
843 Atmospherically Relevant Multicomponent Aerosol Particles. *The Journal of Physical*
844 *Chemistry A*, 119(19), 4489–4497. <https://doi.org/10.1021/jp510268p>
- 845 Lee, A. K. Y., Ling, T. Y., & Chan, C. K. (2008). Understanding hygroscopic growth and phase
846 transformation of aerosols using single particle Raman spectroscopy in an electrodynamic
847 balance. *Faraday Discuss.*, 137, 245–263. <https://doi.org/10.1039/B704580H>

Formatted: Font: (Default) +Body (Aptos), 11 pt, Not Italic

Formatted: Normal, Left

848 Lee, J. Y., & Hildemann, L. M. (2013). Comparisons between Hygroscopic Measurements and
849 UNIFAC Model Predictions for Dicarboxylic Organic Aerosol Mixtures. *Advances in*
850 *Meteorology*, 2013, 1–9. <https://doi.org/10.1155/2013/897170>

851 Lei, T., Su, H., Ma, N., Pöschl, U., Wiedensohler, A., & Cheng, Y. (2023). Size-dependent
852 hygroscopicity of levoglucosan and D-glucose aerosol nanoparticles. *Atmospheric*
853 *Chemistry and Physics*, 23(8), 4763–4774. <https://doi.org/10.5194/acp-23-4763-2023>

854 Li, J., Carlson, B. E., Yung, Y. L., Lv, D., Hansen, J., Penner, J. E., Liao, H., Ramaswamy, V.,
855 Kahn, R. A., Zhang, P., Dubovik, O., Ding, A., Lacis, A. A., Zhang, L., & Dong, Y. (2022).
856 Scattering and absorbing aerosols in the climate system. *Nature Reviews Earth &*
857 *Environment*, 3(6), 363–379. <https://doi.org/10.1038/s43017-022-00296-7>

858 [Li, E. Y., Yazdani, A., Dillner, A. M., Shen, G., Champion, W. M., Jetter, J. J., Preston, W. T.,](#)
859 [Russell, L. M., Hays, M. D., & Takahama, S. \(2024\). Quantifying functional group](#)
860 [compositions of household fuel-burning emissions. *Atmospheric Measurement*](#)
861 [Techniques](#), 17(8), 2401–2413. <https://doi.org/10.5194/amt-17-2401-2024>

Formatted: Line spacing: 1.5 lines

862 ▲
863 Lide, D. R. CRC Handbook of Chemistry and Physics; CRC press, 2004; Vol. 85.

Formatted: Font: (Default) +Body (Aptos), 11 pt

Formatted: Normal, Left

864 Liu, Q., Jing, B., Peng, C., Tong, S., Wang, W., & Ge, M. (2016). Hygroscopicity of internally
865 mixed multi-component aerosol particles of atmospheric relevance. *Atmospheric*
866 *Environment*, 125, 69–77. <https://doi.org/10.1016/j.atmosenv.2015.11.003>

867 Luo, Q., Hong, J., Xu, H., Han, S., Tan, H., Wang, Q., Tao, J., Ma, N., Cheng, Y., & Su, H. (2020).
868 Hygroscopicity of amino acids and their effect on the water uptake of ammonium sulfate
869 in the mixed aerosol particles. *Science of The Total Environment*, 734, 139318.
870 <https://doi.org/10.1016/j.scitotenv.2020.139318>

871 [Ma, Q., Liu, Y., & He, H. \(2010\). The Utilization of Physisorption Analyzer for Studying the](#)
872 [Hygroscopic Properties of Atmospheric Relevant Particles. *The Journal of Physical*](#)
873 [Chemistry A](#), 114(12), 4232–4237. <https://doi.org/10.1021/jp909340v>

Formatted: Line spacing: 1.5 lines

874 ▲
875 Maffia, M. C., & Meirelles, A. J. A. (2001). Water Activity and pH in Aqueous Polycarboxylic
876 Acid Systems. *Journal of Chemical & Engineering Data*, 46(3), 582–587.
877 <https://doi.org/10.1021/je0002890>

Formatted: Font: (Default) +Body (Aptos), 11 pt

Formatted: Normal, Left

878 Marsh, A., Rovelli, G., Miles, R. E. H., & Reid, J. P. (2019). Complexity of Measuring and
879 Representing the Hygroscopicity of Mixed Component Aerosol. *The Journal of Physical
880 Chemistry A*, 123(8), 1648–1660. <https://doi.org/10.1021/acs.jpca.8b11623>

881 [McInnes, L. M., Quinn, P. K., Covert, D. S., & Anderson, T. L. \(1996\). Gravimetric analysis, ionic
882 composition, and associated water mass of the marine aerosol. *Atmospheric Environment*,
883 30\(6\), 869–884. \[https://doi.org/10.1016/1352-2310\\(95\\)00354-1\]\(https://doi.org/10.1016/1352-2310\(95\)00354-1\)](#)

884 [Mikhailov, E. F., Merkulov, V. V., Vlasenko, S. S., Ryshkevich, T. I., & Pöschl, U. J. \(2011\).
885 Filter-based differential hygroscopicity analyzer of aerosol particles. *Izvestiya*,
886 *Atmospheric and Oceanic Physics*, 47\(6\), 747–759.
887 <https://doi.org/10.1134/S0001433811060107>](#)

888 [Mikhailov, E. F., & Vlasenko, S. S. \(2020\). High-humidity tandem differential mobility analyzer
889 for accurate determination of aerosol hygroscopic growth, microstructure, and activity
890 coefficients over a wide range of relative humidity. *Atmospheric Measurement Techniques*,
891 13\(4\), 2035–2056. <https://doi.org/10.5194/amt-13-2035-2020>](#)

893 Mikhailov, E. F., Pöhlker, M. L., Reinmuth-Selzle, K., Vlasenko, S. S., Krüger, O. O., Fröhlich-
894 Nowoisky, J., Pöhlker, C., Ivanova, O. A., Kiselev, A. A., Kremper, L. A., & Pöschl, U.
895 (2021). Water uptake of subpollen aerosol particles: Hygroscopic growth, cloud
896 condensation nuclei activation, and liquid–liquid phase separation. *Atmospheric Chemistry
897 and Physics*, 21(9), 6999–7022. <https://doi.org/10.5194/acp-21-6999-2021>

898 Mikhailov, E. F., Vlasenko, S. S., & Kiselev, A. A. (2024). Water activity and surface tension of
899 aqueous ammonium sulfate and D-glucose aerosol nanoparticles. *Atmospheric Chemistry
900 and Physics*, 24(5), 2971–2984. <https://doi.org/10.5194/acp-24-2971-2024>

901 Mochida, M., & Kawamura, K. (2004). Hygroscopic properties of levoglucosan and related
902 organic compounds characteristic to biomass burning aerosol particles. *Journal of
903 Geophysical Research: Atmospheres*, 109(D21), 2004JD004962.
904 <https://doi.org/10.1029/2004JD004962>

905 Nadler, K. A., Kim, P., Huang, D.-L., Xiong, W., & Continetti, R. E. (2019). Water diffusion
906 measurements of single charged aerosols using H₂O/D₂O isotope exchange and Raman
907 spectroscopy in an electrodynamic balance. *Physical Chemistry Chemical Physics*, 21(27),
908 15062–15071. <https://doi.org/10.1039/C8CP07052K>

Formatted: Line spacing: 1.5 lines

Formatted: Font: (Default) +Body (Aptos), 11 pt

Formatted: Normal, Left

909 Nenes, A., Pandis, S. N., & Pilinis, C. (1998). *ISORROPIA: A New Thermodynamic Equilibrium*
910 *Model for Multiphase Multicomponent Inorganic Aerosols*. *Aquatic Geochemicals* 4, 123–
911 152.

912 Padró, L. T., Moore, R. H., Zhang, X., Rastogi, N., Weber, R. J., & Nenes, A. (2012). Mixing state
913 and compositional effects on CCN activity and droplet growth kinetics of size-resolved
914 CCN in an urban environment. *Atmospheric Chemistry and Physics*, 12(21), 10239–10255.
915 <https://doi.org/10.5194/acp-12-10239-2012>

916 Peng, C., Chen, L., & Tang, M. (2022). A database for deliquescence and efflorescence relative
917 humidities of compounds with atmospheric relevance. *Fundamental Research*, 2(4), 578–
918 587. <https://doi.org/10.1016/j.fmre.2021.11.021>

919 Peng, C., Chow, A. H. L., & Chan, C. K. (2001). Hygroscopic Study of Glucose, Citric Acid, and
920 Sorbitol Using an Electrodynamic Balance: Comparison with UNIFAC Predictions.
921 *Aerosol Science and Technology*, 35(3), 753–758.
922 <https://doi.org/10.1080/02786820152546798>

923 Peng, C., Jing, B., Guo, Y.-C., Zhang, Y.-H., & Ge, M.-F. (2016). Hygroscopic Behavior of
924 Multicomponent Aerosols Involving NaCl and Dicarboxylic Acids. *The Journal of*
925 *Physical Chemistry A*, 120(7), 1029–1038. <https://doi.org/10.1021/acs.jpca.5b09373>

926 Pope, F. D., Dennis-Smith, B. J., Griffiths, P. T., Clegg, S. L., & Cox, R. A. (2010). Studies of
927 Single Aerosol Particles Containing Malonic Acid, Glutaric Acid, and Their Mixtures with
928 Sodium Chloride. I. Hygroscopic Growth. *The Journal of Physical Chemistry A*, 114(16),
929 5335–5341. <https://doi.org/10.1021/jp100059k>

930 Prenni, A. J., DeMott, P. J., Kreidenweis, S. M., Sherman, D. E., Russell, L. M., & Ming, Y.
931 (2001). The Effects of Low Molecular Weight Dicarboxylic Acids on Cloud Formation.
932 *The Journal of Physical Chemistry A*, 105(50), 11240–11248.
933 <https://doi.org/10.1021/jp012427d>

934 Qu, W., Zhang, X., Wang, Y., & Fu, G. (2020). Atmospheric visibility variation over global land
935 surface during 1973–2012: Influence of meteorological factors and effect of aerosol, cloud
936 on ABL evolution. *Atmospheric Pollution Research*, 11(4), 730–743.
937 <https://doi.org/10.1016/j.apr.2020.01.002>

938 Reich, O., Gleichweit, M. J., David, G., Leemann, N., & Signorell, R. (2023). Hygroscopic growth
939 of single atmospheric sea salt aerosol particles from mass measurement in an optical trap.

940 *Environmental Science: Atmospheres*, 3(4), 695–707.
941 <https://doi.org/10.1039/D2EA00129B>

942 Ruthenburg, T. C., Perlin, P. C., Liu, V., McDade, C. E., & Dillner, A. M. (2014). Determination
943 of organic matter and organic matter to organic carbon ratios by infrared spectroscopy
944 with application to selected sites in the IMPROVE network. *Atmospheric Environment*,
945 86, 47–57. <https://doi.org/10.1016/j.atmosenv.2013.12.034>

Formatted: Line spacing: 1.5 lines

946 Saxena, P., Hildemann, L. M., McMurry, P. H., and Seinfeld, J. H.: Organics alter hygroscopic
947 behavior of atmospheric particles. *J. Geophys. Res.*, 100D, 18 755–18 770, 1995

Formatted: Font: (Default) +Body (Aptos), 11 pt

Formatted: Normal, Left

Formatted: Space After: 0 pt

948 Shearman, R.W. and Menzies, A.W.C. (1937) The Solubilities of Potassium Chloride in
949 Deuterium Water and in Ordinary Water from 0 to 180⁰. *J. Am. Chem. Soc.*, 59: 185.

951 Shingler, T., Crosbie, E., Ortega, A., Shiraiwa, M., Zuend, A., Beyersdorf, A., Ziemba, L.,
952 Anderson, B., Thornhill, L., Perring, A. E., Schwarz, J. P., Campazano-Jost, P., Day, D.
953 A., Jimenez, J. L., Hair, J. W., Mikoviny, T., Wisthaler, A., & Sorooshian, A. (2016).
954 Airborne characterization of subsaturated aerosol hygroscopicity and dry refractive index
955 from the surface to 6.5 km during the SEAC⁴ RS campaign. *Journal of Geophysical*
956 Research: Atmospheres, 121(8), 4188–4210. <https://doi.org/10.1002/2015JD024498>

Formatted: Line spacing: 1.5 lines

957
958 Sjogren, S., Gysel, M., Weingartner, E., Baltensperger, U., Cubison, M. J., Coe, H., Zardini, A.
959 A., Marcolli, C., Krieger, U. K., & Peter, T. (2007). Hygroscopic growth and water uptake
960 kinetics of two-phase aerosol particles consisting of ammonium sulfate, adipic and humic
961 acid mixtures. *Journal of Aerosol Science*, 38(2), 157–171.
962 <https://doi.org/10.1016/j.jaerosci.2006.11.005>

963 Solomon, P. A., Crumpler, D., Flanagan, J. B., Jayanty, R. K. M., Rickman, E. E., & McDade, C.
964 E. (2014). U.S. National PM_{2.5} Chemical Speciation Monitoring Networks—CSN and
965 IMPROVE: Description of networks. *Journal of the Air & Waste Management*
966 Association, 64(12), 1410–1438. <https://doi.org/10.1080/10962247.2014.956904>

Formatted: Line spacing: 1.5 lines

967 Sorooshian, A., Hersey, S., Brechtel, F. J., Corless, A., Flagan, R. C., & Seinfeld, J. H. (2008).
968 Rapid, Size-Resolved Aerosol Hygroscopic Growth Measurements: Differential Aerosol

969 [Sizing and Hygroscopicity Spectrometer Probe \(DASH-SP\). *Aerosol Science and*](#)
970 [Technology](#), 42(6), 445–464. <https://doi.org/10.1080/02786820802178506>

971 ▲
972 Steimer, S. S., Krieger, U. K., Te, Y.-F., Lienhard, D. M., Huisman, A. J., Ammann, M., & Peter,
973 T. (2015). *Electrodynamic balance measurements of thermodynamic, kinetic, and optical*
974 *aerosol properties inaccessible to bulk methods*. <https://doi.org/10.5194/amtd-8-689-2015>

975 [Takahama, S., Dillner, A. M., Weakley, A. T., Reggente, M., Bürki, C., Lbadaoui-Darvas, M.,](#)
976 [Debus, B., Kuzmiakova, A., & Wexler, A. S. \(2019\). Atmospheric particulate matter](#)
977 [characterization by Fourier transform infrared spectroscopy: A review of statistical](#)
978 [calibration strategies for carbonaceous aerosol quantification in US measurement](#)
979 [networks. *Atmospheric Measurement Techniques*, 12\(1\), 525–567.](#)
980 <https://doi.org/10.5194/amt-12-525-2019>

981 ▲
982 Tang, I. N., & Munkelwitz, H. R. (1991). Simultaneous Determination of Refractive Index and
983 Density of an Evaporating Aqueous Solution Droplet. *Aerosol Science and Technology*,
984 15(3), 201–207. <https://doi.org/10.1080/02786829108959527>

985 [Tang, M., Chan, C.K., Li, Y.J., Su, H., Ma, O., Wu, Z., Zhang, G., Wang, Z., Ge, M., Hu, M., He,](#)
986 [H., Wang, X. \(2019\) A review of experimental techniques for aerosol hygroscopicity](#)
987 [studies. *Atmospheric Chemistry and Physics*, 19\(19\), 12631–12686.](#)
988 <https://doi.org/10.5194/acp-19-12631-2019>

989 ▲
990 Topping, D., Barley, M., Bane, M. K., Higham, N., Aumont, B., Dingle, N., & McFiggans, G.
991 (2016). UManSysProp v1.0: An online and open-source facility for molecular property
992 prediction and atmospheric aerosol calculations. *Geoscientific Model Development*, 9(2),
993 899–914. <https://doi.org/10.5194/gmd-9-899-2016>

994 Wang, J., Cubison, M. J., Aiken, A. C., Jimenez, J. L., & Collins, D. R. (2010). The importance of
995 aerosol mixing state and size-resolved composition on CCN concentration and the variation
996 of the importance with atmospheric aging of aerosols. *Atmospheric Chemistry and Physics*,
997 10(15), 7267–7283. <https://doi.org/10.5194/acp-10-7267-2010>

Formatted: Font: (Default) +Body (Aptos), 11 pt

Formatted: Normal, Left

Formatted: Font: (Default) +Body (Aptos), 11 pt

Formatted: Normal, Left

Formatted: Font: (Default) +Body (Aptos), 11 pt

Formatted: Normal, Left

- 998 Wang, K., Huang, R.-J., Brüggemann, M., Zhang, Y., Yang, L., Ni, H., Guo, J., Wang, M., Han,
999 J., Bilde, M., Glasius, M., & Hoffmann, T. (2021). Urban organic aerosol composition in
1000 eastern China differs from north to south: Molecular insight from a liquid chromatography–
1001 mass spectrometry (Orbitrap) study. *Atmospheric Chemistry and Physics*, *21*(11), 9089–
1002 9104. <https://doi.org/10.5194/acp-21-9089-2021>
- 1003 Wang, X., Shi, Q., Zhao, Y., Wang, X., & Zheng, Y. (2013). MOISTURE ADSORPTION
1004 ISOTHERMS AND HEAT OF SORPTION OF *AGARICUS BISPORUS*: ADSORPTION
1005 ISOTHERMS OF *AGARICUS BISPORUS*. *Journal of Food Processing and Preservation*,
1006 *37*(4), 299–305. <https://doi.org/10.1111/j.1745-4549.2011.00649.x>
- 1007 Wexler, A. and Hasegawa, S., 1954. Relative Humidity-Temperature Relationships of Some
1008 Saturated Salt Solutions in the Temperature Range 0°C to 50°C. *Journal of Research of the*
1009 *National Bureau of Standards*, *53*, 19-26. <https://doi.org/10.6028/jres.053.003>
- 1010 Wexler, A. S., & Seinfeld, J. H. (1991). Second-generation inorganic aerosol model. *Atmospheric*
1011 *Environment. Part A. General Topics*, *25*(12), 2731–2748. [https://doi.org/10.1016/0960-](https://doi.org/10.1016/0960-1686(91)90203-J)
1012 [1686\(91\)90203-J](https://doi.org/10.1016/0960-1686(91)90203-J)
- 1013 [White, W. H., Trzepla, K., Hyslop, N. P., & Schichtel, B. A. \(2016\). A critical review of filter](#)
1014 [transmittance measurements for aerosol light absorption, and de novo calibration for a](#)
1015 [decade of monitoring on PTFE membranes. *Aerosol Science and Technology*, *50*\(9\), 984–](#)
1016 [1002. <https://doi.org/10.1080/02786826.2016.1211615>](#)
- 1017 [Yazdani, A., Dillner, A. M., & Takahama, S. \(2021\). Estimating mean molecular weight, carbon](#)
1018 [number, and OM/OC with mid-infrared spectroscopy in organic particulate matter](#)
1019 [samples from a monitoring network. *Atmospheric Measurement Techniques*, *14*\(7\),](#)
1020 [4805–4827. <https://doi.org/10.5194/amt-14-4805-2021>](#)
- 1021
- 1022 Zamora, I. R., & Jacobson, M. Z. (2013). Measuring and modeling the hygroscopic growth of two
1023 humic substances in mixed aerosol particles of atmospheric relevance. *Atmospheric*
1024 *Chemistry and Physics*, *13*(17), 8973–8989. <https://doi.org/10.5194/acp-13-8973-2013>
- 1025 Zamora, I. R., Tabazadeh, A., Golden, D. M., & Jacobson, M. Z. (2011). Hygroscopic growth of
1026 common organic aerosol solutes, including humic substances, as derived from water
1027 activity measurements: WATER ACTIVITY OF ORGANIC AEROSOLS. *Journal of*

Formatted: Line spacing: 1.5 lines

Formatted: Font: (Default) +Body (Aptos), 11 pt

Formatted: Normal, Left

1028 *Geophysical Research: Atmospheres*, 116(D23), n/a-n/a.
1029 <https://doi.org/10.1029/2011JD016067>
1030 Zieger, P., Väisänen, O., Corbin, J. C., Partridge, D. G., Bastelberger, S., Mousavi-Fard, M.,
1031 Rosati, B., Gysel, M., Krieger, U. K., Leck, C., Nenes, A., Riipinen, I., Virtanen, A., &
1032 Salter, M. E. (2017). Revising the hygroscopicity of inorganic sea salt particles. *Nature*
1033 *Communications*, 8(1), 15883. <https://doi.org/10.1038/ncomms15883>
1034 Zuend, A., Marcolli, C., Peter, T., & Seinfeld, J. H. (2010). Computation of liquid-liquid equilibria
1035 and phase stabilities: Implications for RH-dependent gas/particle partitioning of organic-
1036 inorganic aerosols. *Atmospheric Chemistry and Physics*, 10(16), 7795–7820.
1037 <https://doi.org/10.5194/acp-10-7795-2010>

1038
|

Formatted: Line spacing: 1.5 lines